The Chromatin and Transcriptional Landscape of Native *Saccharomyces cerevisiae* Telomeres and Subtelomeric Domains

Aisha Ellahi,[1] Deborah M. Thurtle,[1] and Jasper Rine[2]
Department of Molecular and Cell Biology, California Institute for Quantitative Biosciences, University of California at Berkeley, Berkeley, California 94720

ABSTRACT *Saccharomyces cerevisiae* telomeres have been a paradigm for studying telomere position effects on gene expression. Telomere position effect was first described in yeast by its effect on the expression of reporter genes inserted adjacent to truncated telomeres. The reporter genes showed variable silencing that depended on the Sir2/3/4 complex. Later studies examining subtelomeric reporter genes inserted at natural telomeres hinted that telomere position effects were less pervasive than previously thought. Additionally, more recent data using the sensitive technology of chromatin immunoprecipitation and massively parallel sequencing (ChIP-Seq) revealed a discrete and noncontinuous pattern of coenrichment for all three Sir proteins at a few telomeres, calling the generality of these conclusions into question. Here we combined the ChIP-Seq of the Sir proteins with RNA sequencing (RNA-Seq) of messenger RNAs (mRNAs) in wild-type and in *SIR2*, *SIR3*, and *SIR4* deletion mutants to characterize the chromatin and transcriptional landscape of all native *S. cerevisiae* telomeres at the highest achievable resolution. Most *S. cerevisiae* chromosomes had subtelomeric genes that were expressed, with only ~6% of subtelomeric genes silenced in a *SIR*-dependent manner. In addition, we uncovered 29 genes with previously unknown cell-type-specific patterns of expression. These detailed data provided a comprehensive assessment of the chromatin and transcriptional landscape of the subtelomeric domains of a eukaryotic genome.

KEYWORDS Sir complex; telomeres; ChIP-Seq; RNA-Seq; mating-type regulation

TELOMERES are specialized structures at the ends of eukaryotic chromosomes that are critical for various biological functions. Telomeres bypass the problem of replicating the ends of linear DNA, protect chromosome ends from exonucleases and nonhomologous end joining, prevent the linear DNA ends from activating a DNA-damage checkpoint, and exhibit suppressed recombination [reviewed in Wellinger and Zakian (2012)]. In *Saccharomyces cerevisiae*, telomeres are composed of three sequence features: telomeric repeats, which consist of 300 ± 75 bp of $(TG_{1-3})_n$ repeated units produced by telomerase; X elements; and Y′ elements, which contain an ORF for a putative helicase gene. The X elements are subdivided into a core X [consisting of an autonomously replicating sequence (ARS) consensus sequence and an Abf1-binding site] and subtelomeric repeats that have variable numbers of repeated units containing a binding site for Tbf1 (Louis 1995). All telomeres contain telomeric repeats plus an X element, and about half of *S. cerevisiae*'s 32 telomeres also contain a Y′ element (X-Y′ telomeres). X-only telomeres contain an X element but not a Y′ element. Unlike the Y′ elements, the telomeric repeats and X elements are bound by proteins that are critical for maintenance of telomeres. Rap1 binds the TG_{1-3} telomeric repeats and recruits the Sir2/3/4 protein complex, the trio of heterochromatin structural proteins critical for repression of the silent mating loci *HML*α and *HMR***a**. Sir proteins are also recruited to the core X sequence through interactions with Abf1 and the origin recognition complex (ORC), which binds the ARS consensus sequence within the core X. Thus telomeres have a heterogeneous sequence composition, recruit proteins that can form heterochromatin-like structures, and are critical for maintaining the genomic integrity of the cell.

doi: 10.1534/genetics.115.175711
Manuscript received February 19, 2015; accepted for publication March 22, 2015; published Early Online March 30, 2015.
Supporting information is available online at www.genetics.org/lookup/suppl/doi:10.1534/genetics.115.175711/-/DC1
[1]These authors contributed equally to this work.
[2]Corresponding author: 374A Stanley Hall, University of California at Berkeley, Berkeley, California 94720-3220. E-mail: jrine@berkeley.edu

As first described in *Drosophila* (Schultz 1947; Hazelrigg *et al.* 1984), the heterochromatic structure of telomeric chromatin results in the transcriptional silencing of adjacent genes, an effect known as *telomere position effect*. Since its description, telomere position effect has been observed in other organisms, where it can be an important means of regulating gene expression. For example, the malarial parasite *Plasmodium falciparum* genome contains subtelomeric *var* genes that encode cell surface antigens that use Sir2-dependent telomeric heterochromatin for their repression (Guizetti and Scherf 2013). *var* genes are selectively expressed, one at a time, and switch expression states, allowing *Plasmodium* to stay ahead of the host's immune response. This selective expression of one antigen over all the other antigen genes is maintained by the epigenetic silencing of all *var* copies except the expressed one (Tonkin *et al.* 2009; Guizetti and Scherf 2013). Similarly, in *Candida glabrata*, the *EPA* adhesion genes essential for colonization of the host urinary tract are located in subtelomeric regions, and their expression is regulated by a Sir-protein-based silencing mechanism that is responsive to the differences in niacin concentration in the bloodstream *vs.* the urinary track (De Las Peñas *et al.* 2003; Domergue *et al.* 2005). In *S. cerevisiae*, genes encoding cell wall components and genes required for the metabolism of certain nutrients tend to be located in subtelomeric regions and are expressed specifically under certain stressful conditions (Ai *et al.* 2002).

Telomere position effect was first described in *S. cerevisiae* by the attenuated expression of reporter genes placed adjacent to a synthetic telomere on either the left arm of chromosome VII or the right arm of chromosome V (Gottschling *et al.* 1990; Renauld *et al.* 1993; Fourel *et al.* 1999). Reminiscent of general epigenetic silencing, the effect was concluded to be independent of gene identity and promoter sequence. Furthermore, much like silencing at the mating-type cassettes *HMLα* and *HMRa*, the silenced state of telomere-adjacent *URA3* and *ADE2* was heritable and depended on the *s*ilent *i*nformation *r*egulator proteins Sir2, Sir3, and Sir4. Unlike *HMLα* and *HMRa*, deletion of *SIR1* had no effect on telomeric silencing (Aparicio *et al.* 1991). These and other early studies led to the view that Sir proteins were in a continuous gradient, highest at the telomere and extending inward for a few kilobase pairs, depending in particular on the level of Sir3 protein (Renauld *et al.* 1993; Hecht *et al.* 1996; Strahl-Bolsinger *et al.* 1997).

More recent findings have questioned the earlier view of telomere position effect in *S. cerevisiae*. For example, when inserted adjacent to the native telomeres *TEL10R*, *TEL04L*, and *TEL03R*, the same *URA3* reporter detects little transcriptional repression (Pryde and Louis 1999). For the few natural telomeres at which *URA3* appears repressed (*TEL13R*, *TEL11L*, and *TEL02R*), silencing is discontinuous across the length of the telomere and largely restricted to positions close to the X element. Similarly, Sir proteins also associate discretely at select natural telomeres, with the highest levels of enrichment proximal to the X element (Zill *et al.* 2010; Radman-Livaja *et al.* 2011; Thurtle and Rine 2014). The natural telomeres that repress the *URA3* transgene exhibit a characteristic array of phased nucleosomes specific to those telomeres (Loney *et al.* 2009). Additionally, some Y′ elements are transcribed, a fact that is inconsistent with Sir protein–mediated repression of all Y′ elements (Fourel *et al.* 1999; Pryde and Louis 1999). In addition to these discrepancies, metabolic reporters are not biologically neutral, and some complexity regarding these reporters has emerged (Rossmann *et al.* 2011; Takahashi *et al.* 2011). For example, *DOT1*, *SWI4*, and *ARD1*, all of which abrogate H3K79 methylation, had been implicated in telomeric silencing, as assayed by the *URA3* reporter at artificial telomeres. However, transcription of native genes at telomeres, as measured by microarray analysis, revealed little change in expression level in a *dot1* mutant and other mutants proposed to disrupt H3K79 methylation (Takahashi *et al.* 2011). Subsequent interrogation of the *URA3* reporter found that *dot1* and other mutants are actually differentially sensitized to the drug 5-FOA used to monitor *URA3* expression (Rossmann *et al.* 2011). Therefore, the phenotypes of these mutants, as measured by 5-FOA sensitivity, do not reliably reflect the transcriptional status of *URA3* at telomeres.

In summary, establishing the prevalence of telomere position effect and identifying the genes and proteins that mediate it have been complicated by three issues: (1) nonsystematic studies of different telomeres in *S. cerevisiae*, (2) the influence of metabolism on telomeric reporters, and (3) limitations on the resolution of chromatin immunoprecipitation (ChIP) and microarray analysis. To resolve these confounding issues, we undertook a high-resolution analysis of chromatin architecture and expression state at all natural *S. cerevisiae* telomeres, free of reporter genes, by using chromatin immunoprecipitation and massively parallel sequencing (ChIP-Seq) analysis of Sir proteins combined with RNA sequencing (RNA-Seq) analysis of wild-type (WT) cells and *sir2Δ*, *sir3Δ*, and *sir4Δ* mutants. ChIP-Seq of acetylated H4K16, a histone mark anticorrelated with silencing, was also analyzed to further evaluate specific histone modifications with respect to expression data from RNA-Seq. This study provided a definitive analysis of the chromatin landscape and degree of silencing at telomeres in *S. cerevisiae* and highlighted the functional variation among telomeres, befitting the accelerated sequence changes seen in these cauldrons of genetic innovation.

Materials and Methods

Yeast strains

Yeast strains and plasmid-containing strains are listed in Supporting Information, Table S5. All yeast strains were generated in the W303 background. Deletion alleles were constructed via one-step integration of knockout cassettes (Longtine *et al.* 1998).

RNA isolation

Cells were grown at 30° in rich medium (YPD) to an A_{600} of 0.8. RNA was extracted from 15 A_{600} units of cells using the hot acid–phenol and chloroform method (Collart and Oliviero 2001). Briefly, cells were incubated in TES buffer (10 mM Tris HCl, pH 7.5, 10 mM EDTA, and 0.5% SDS) and citrate-saturated phenol (pH 4.3) for 1 hr at 65° and vortexed every 10 min. RNA was isolated from lysed cells with two rounds of phenol-chloroform extraction, pelleted, and then resuspended in RNase-free water and treated with DNase I (Roche) to digest genomic DNA. A final round of phenol-chloroform extraction was performed prior to library preparation and/or complementary DNA (cDNA) synthesis.

RNA library preparation and sequencing

Paired-end sequencing was performed to accurately assign reads. 100-bp paired-end RNA-Seq libraries were prepared using the Illumina TruSeq Stranded mRNA Sample Prep Kit with 4 μg of total RNA as starting material, as described in the TruSeq Stranded mRNA Sample Prep Kit protocol. Libraries were quantified using a Bioanalyzer (Agilent) and sequenced on an Illumina HiSeq 2000 machine. Reads have been deposited in the NCBI Sequence Read Archive (SRA) at http://www.ncbi.nlm.nih.gov/sra under accession no. SRP055208.

Quantitative reverse-transcriptase-PCR (qRT-PCR) analysis

cDNA was prepared from 2 μg of total RNA using the SuperScript III Reverse Transcriptase Kit (Invitrogen). qRT-PCR was performed using SYBR Green Real-Time PCR Master Mix (Thermofisher) and was quantified using a Stratagene Mx3000 qPCR System. Standard curves were generated from a WT strain and a *sir2Δ* strain, and all expression values were normalized to *ACT1*. Values shown are the average of three biological replicates. Error bars reflect the standard error. Two-tailed Student's *t*-test was performed to evaluate the significance of the observed differences in expression. Oligos used are listed in Table S6.

Data analysis

ChIP-Seq read mapping: ChIP-Seq reads analyzed were from previous Sir protein ChIP studies (Teytelman *et al.* 2013; Thurtle and Rine 2014), deposited in the NCBI Sequence Read Archive under accession nos. SRP030670 and SRP034921, respectively. Reads were mapped using BWA (Li and Durbin 2009) to a modified sacCer2 genome in which the *MAT* locus was replaced with the Hyg-MX cassette. Duplicate reads were removed using Picard (http://picard.sourceforge.net). Because of the repeated sequences shared among telomeres, some reads could not be mapped to specific telomeres. Making the simplifying assumption that all copies of a repeat sequence contributed to the production of sequence reads of that repeat, reads that mapped to repeated sequences were randomly assigned to copies of that repeat, allowing for an estimation of Sir protein association even at the repetitive elements of the telomeres. However, to indicate which reads were uniquely mapped and which mapped more than once, we graphed the percentage of reads within each telomere that did not map uniquely (Figure S3). This analysis clearly showed that Y′ elements at all telomeres are difficult to distinguish from each other except at positions of polymorphisms unique to individual Y′ elements. Additionally, almost the entire 20-kbp regions of *TEL01R*, *TEL04L*, *TEL09L*, *TEL10L*, *TEL10R*, *TEL14L*, *TEL15R*, and *TEL16L* are not unique. The laboratory strain (derived from W303) on which the ChIP-Seq experiments were performed had deletions in subtelomeric regions compared to the S288C reference genome (*TEL07L*, *TEL14R*, and small gaps on *TEL01R* and *TEL13R*). These missing regions in the sequenced strain were indicated in the figures. Reads were mapped to the S288C genome to allow direct reference to the annotated features on the *Saccharomyces* Genome Database (SGD). For each sample, per-base-read counts were determined using SAMtools (Li *et al.* 2009). Enrichment was determined as the number of IP reads divided by the number of input reads for that base-pair position.

MACS peak calling: MACS peak calling was performed on the default settings, except that no model was used to optimize for the broader peaks typical of chromatin-interacting proteins. For each Sir protein chromatin sample, MACS was run on two biological replicates of ChIP-Seq data from chromatin sheared by sonication and on a third sample for each Sir protein in which the chromatin sample was prepared by enzymatic digestion with MNase (Thurtle and Rine 2014). For each chromatin sample analyzed with MACS, the IP sample was the "treatment," and the input sample was the "control." We defined peaks as reproducible if they were called in at least two of the three data sets, as noted in Table S1.

RNA-Seq: Reads were mapped using Tophat2, and per-gene transcript quantification was performed using Cufflinks and reported as *f*ragments *p*er *k*ilobase per *m*illion reads (FPKM) (Trapnell *et al.* 2009, 2012). Locations of multi-mapped RNA reads are indicated in Figure S8. Genome-wide RNA read pileups per base pair were calculated using SAMtools (Li *et al.* 2009). The DESeq pipeline was used to perform differential gene expression analysis, as outlined in the following steps: (1) raw read counts per gene were determined using htseq-count, which discards multimapped paired-end read fragments (Anders and Huber 2010); therefore, only uniquely mapped reads were included in tests for differential expression of genes; and (2) read counts were normalized and subjected to differential expression analysis using the DESeq package in R (Anders and Huber 2013). Genes that showed statistically significant differences in expression of twofold or greater relative to WT with a *P*-value of less than 0.05 and a false-discovery rate of less than 10% were included in the final list of

candidate genes under *SIR2/3/4* repression or as possible haploid-specific genes.

Comparison of transcription at telomeres vs. nontelomeric loci: Genes were classified as either falling within (telomeric) or not falling within (nontelomeric) 20 kbp of a chromosome end, resulting in two distributions of FPKM values. A Wilcoxon rank-sum test was performed to compare the telomeric *vs.* nontelomeric distributions.

MEME analysis: The MAST program within the MEME package was used to scan the coding sequence, plus and minus 1000 base pairs, for a1/α2 and α2/Mcm1 binding sites in candidate haploid-specific genes (Bailey *et al.* 2009). Results were filtered for *E*-values < 10.

Scanning motif binding sites on the yeast transcription factor specificity compendium: The Binding Site Genome Browser (http://nbrowse.ccbr.utoronto.ca/mgb2/gbrowse/yetfasco/) was used to search for a1/α2 and α2/Mcm1 binding sites within 1 kbp of each candidate gene. All a1/α2 and α2 binding sites with a score greater than 80% of the motif's maximum position-weighted matrix-score threshold were noted.

Results

Sir proteins associated at discrete positions at natural telomeres

To investigate Sir protein association at the 32 natural telomeres of *S. cerevisiae*, we analyzed ChIP-Seq data sets in the 20-kbp subtelomeric region of Myc-tagged Sir2, Sir3, and Sir4 from our previous Sir ChIP-Seq studies (Thurtle and Rine 2014) (Figure 1). Additionally, we analyzed ChIP-Seq data sets for green fluorescent protein endowed with a nuclear localization signal (GFP-NLS) and a no-tag sample immunoprecipitated with the Myc antibody as controls for artifacts of ChIP-Seq analyses and nonspecific enrichment, respectively (Teytelman *et al.* 2013) (Figure S1 and Figure S2). The telomeric regions are difficult to analyze because of their repetitive nature and incomplete sequencing at some of the telomere ends. Thus we made simplifying assumptions about ambiguously mapped reads, as outlined in *Materials and Methods* and Figure S3. The peaks at the *TEL05L* and *TEL14L* chromosomes, for example, for which no telomeric repeats are annotated, presumably arose from ChIP-Seq reads that extended from telomeric repeats into sufficiently unique flanking sequences to allow mapping. Where the telomerase-generated repeats are present, the Rap1 protein-binding sites embedded in those repeats were presumably responsible for the Sir protein enrichment at those positions (*e.g.*, *TEL08R* and *TEL08L*). Most strikingly, at the 32 natural telomeres, the enrichment patterns of the three Sir protein complex members were highly similar, illustrating both the remarkable degree of reproducibility of the enrichment patterns and the discontinuous nature of the Sir protein enrichments at each and every telomere (Figure 1). There was no evidence of a gradient of Sir proteins, as envisioned by early models of telomere position effect (Hecht *et al.* 1996). The discontinuous distribution of Sir proteins has been reported previously for specific telomeres (Zill *et al.* 2010; Thurtle and Rine 2014). Overall, this analysis clearly established the generality of the discrete nature of Sir protein association at all 32 telomeres.

To provide a statistical evaluation of the Sir2, Sir3, and Sir4 peaks detected by eye, we called peaks of significant enrichment with MACS using the default *P*-value cutoff of 0.00001 (Zhang *et al.* 2008). To control for nonspecific enrichment, we also called peaks of enrichment with MACS on a ChIP-Seq data set from a heterologous protein control, GFP-NLS. For the GFP-NLS, only one small region on the *TEL02L* (base-pair positions 8824–10,250) showed overlapping enrichment with Sir protein peaks. Thus the Sir protein peak was adjusted to account for this nonspecific enrichment. Otherwise, nonspecific enrichment from highly expressed transcripts did not confound the ChIP enrichment at telomeres, in contrast to other places in the genome (Teytelman *et al.* 2013). As determined by the MACS peak calling, all but 5 of the 32 yeast telomere X elements exhibited significant enrichment of Sir proteins (Table S1). For those five telomeres in which MACS did not identify a peak (*TEL1R*, *TEL2R*, *TEL10R*, *TEL13R*, and *TEL14R*), there appeared to be ample enrichment by eye (Figure 1). All five of these telomeres were X-only telomeres in which the enrichment abutted the end of the chromosome, possibly resulting in MACS not calling the peak because of its abrupt end and the presence of a repetitive sequence. Hence Sir protein enrichment appeared to be a property of all, or nearly all, X elements. For 15 of the 19 X-Y′ telomeres, MACS positioned the peak of Sir protein enrichment as extending all the way from the chromosome end to the internal X element, spanning the entire Y′ element (Table S1). To determine whether there actually was detectable Sir protein enrichment within the Y′ element or whether these large peaks called were due to the proximity of two distinct peaks, we calculated the average enrichment (IP/input) for all the X elements and all the Y′ elements for Sir2, Sir3, and Sir4 (Figure S4). For the three Sir proteins, the average X element enrichment was fourfold for Sir2 and eightfold for Sir3 and Sir4. In contrast, the Y′ elements all showed IP/input values of less than 1 for all three Sir proteins, indicating that the IP values for this region all were below background. Thus, as reported previously for specific telomeres (Zhu and Gustafsson 2009; Zill *et al.* 2010; Takahashi *et al.* 2011; Thurtle and Rine 2014), the Y′ elements did not exhibit any Sir protein enrichment. In summary, Sir proteins showed the highest level of association at the core X element, with average enrichment values between 4.5 and 8.2 for the three Sir proteins, where ORC and Abf1 bind, whether at an X-element-only telomere or at an X-Y′ telomere (Figure 1 and Figure S4).

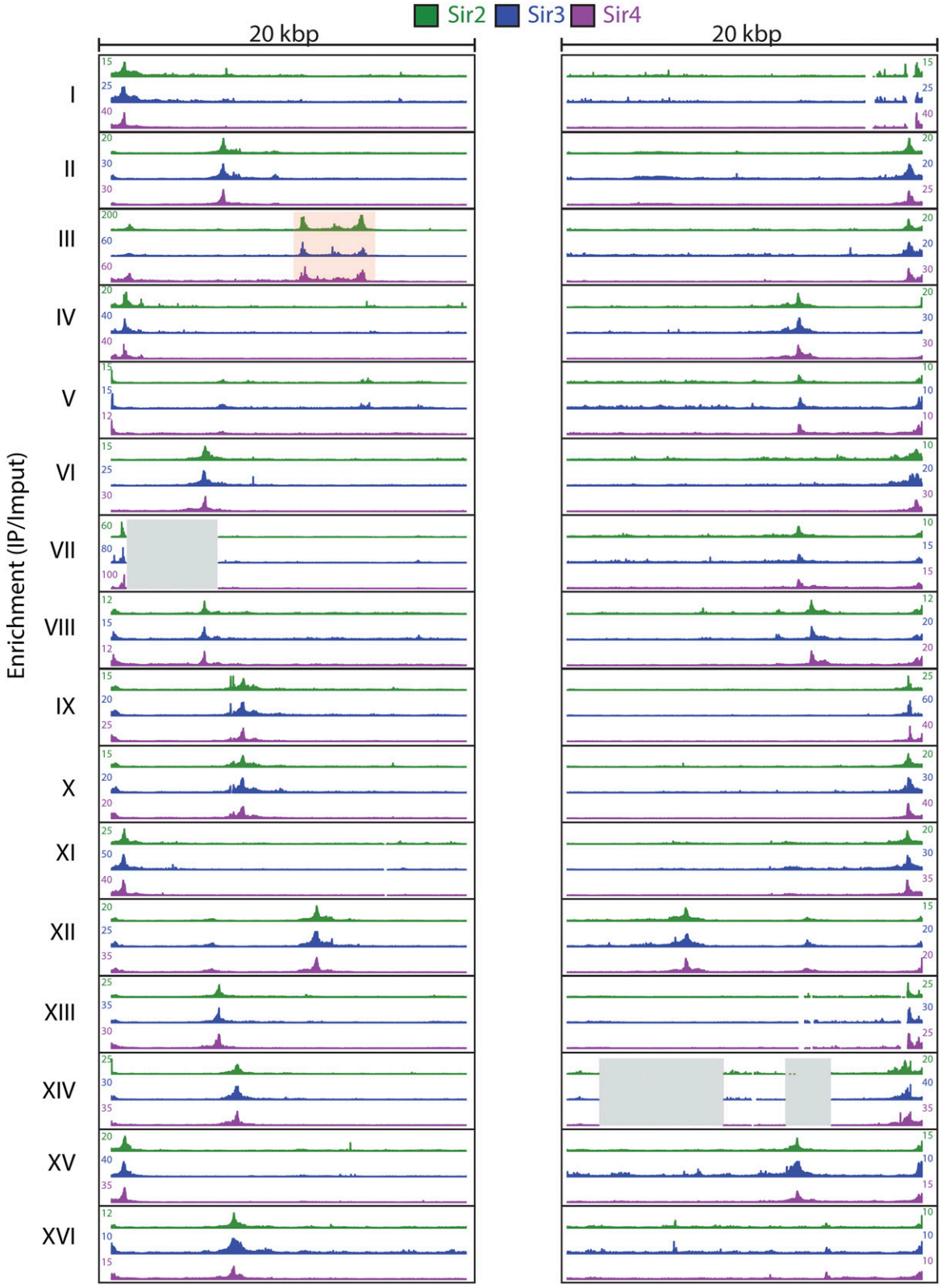

Figure 1 Sir2, Sir3, and Sir4 enrichment at all 32 yeast telomeres. ChIP-Seq of Myc-tagged Sir2, Sir3, and Sir4 was analyzed at all yeast telomeres. (Left) The first 20 kbp of each chromosome. (Right) The last 20 kbp of each chromosome. IP/input enrichment values for Sir2 (green), Sir3 (blue), and Sir4 (green) are shown for each telomere. On chromosome III, *HML* is boxed in red, and regions absent in the sequenced W303 strain relative to the S288C sacCer2 genome are represented by a gray-shaded box.

Catalytic activity of Sir2 at telomeres

To determine whether positions of H4K16 hypoacetylation overlapped with Sir2 distribution at telomeres, we analyzed ChIP-Seq of H4K16-acetyl and compared Sir2 ChIP-Seq profiles at all 32 telomeres to the H4K16-acetyl ChIP-Seq profiles (Figure 2). H4K16 was hypoacetylated in regions slightly larger than the X element, with the lowest levels of H4K16-acetyl at the core X sequence. Additionally, X-Y′ telomeres showed a variable amount of H4K16 hypoacetylation within the Y′ region. We also observed regions of H4K16 hypoacetylation without detectable Sir2 association, which presumably reflected the action of a different histone deacetylase such as Rpd3 or Hst1. Both have been shown to associate with subtelomeric chromatin (Kurdistani *et al.* 2002; Ehrentraut *et al.* 2010; Li *et al.* 2013). Alternatively, the hyopacetylation of H4K16 in these regions could be due to transient Sir2 association not captured by ChIP-Seq. Previous studies have shown that Sir2, but not Sir3 or Sir4, controls some origins of replication (Pappas *et al.* 2004; Crampton *et al.* 2008; Yoshida *et al.* 2014). However, MACS did not detect any significant enrichment for Sir2 at subtelomeric ARSs outside the core X element.

The deacetylation of H4K16-acetyl by Sir2 is thought to be key for the spreading of Sir proteins (Hecht *et al.* 1996; Rusche *et al.* 2002; Hoppe *et al.* 2002). In the standard model for spreading [reviewed in Rusche *et al.* (2002)], Sir proteins are recruited to nucleation sites via protein interactions among ORC, Abf1, and Rap1, which are bound to DNA, Sir3, and a Sir2-Sir4 dimer. According to the model, Sir2 deacetylates nearby nucleosomes, which creates high-affinity binding sites for Sir3 and Sir4, resulting in the spread of additional copies of the Sir protein complex. Thus this model predicts that Sir protein enrichment should be continuously distributed along the length of a telomere. However, the distribution of Sir proteins at the telomeres was discrete (Figure 1 and Figure 2) and therefore not in support of the spreading model. To determine the role of Sir2's catalytic activity in Sir protein association at the telomeres, Sir3 and Sir4 enrichment was examined at the telomeres in a strain lacking Sir2 catalytic activity (Thurtle and Rine 2014). As shown for a representative X-only telomere (*TEL15L*), there seemed to be some indications of spreading for Sir3 because the association of Sir3 in the WT background extended about 800 bp beyond where Sir3 associated in a strain lacking Sir2 catalytic activity (Figure 3). This extended distribution was less prominent for Sir4 at the X-only telomere and both Sir3 and Sir4 at the internal X element of the X-Y′ telomere (*TEL09L*) (Figure 3). These results indicate that if Sir complex spreading occurred at telomeres, it did so only to a slight extent. The prominent feature of all telomeres was the overall reduced Sir3 and Sir4 association at the core X element in a strain lacking Sir2 catalytic activity, indicating that Sir2's catalytic activity is necessary for the association and/or stability of the Sir protein complex with ORC and Abf1. Both Sir3 and Sir4 showed enrichment in the telomeric repeats in a strain lacking Sir2 catalytic activity. However, as reported previously (Zill *et al.* 2010; Teytelman *et al.* 2013), the telomeric repeats showed enrichment in the no-tag ChIP-Seq control sample as well, indicating that the telomeric repeats, whether at the chromosome ends of X-only telomeres or at internal locations of X-Y′ telomeres, interact nonspecifically with the anti-Myc antibody (Figure S2). This interaction seemed to be specific for the Myc antibody because the GFP-NLS immunoprecipitated with an anti-GFP antibody did not show enrichment at the telomeric repeats (Figure S1). It was surprising that the no-tag ChIP-Seq control sample and the Sir3 and Sir4 samples in strains lacking Sir2 catalytic activity indicated greater enrichment at the telomeric repeats than the level of Sir protein enrichment at the telomeric repeats in WT strains. However this apparent greater enrichment may be a consequence of increasing the signal-to-noise ratio: there are fewer sites with lower amounts of Sir3 and Sir4 enrichment in a strain lacking Sir2 catalytic activity and very little association in the no-tag sample; thus more Myc antibody is available to associate nonspecifically with the telomeric repeats. Overall, Sir2's catalytic activity at telomeres was important for association of the Sir protein complex at the core X nucleation sites and less implicated in the spreading of the Sir complex into subtelomeric regions.

Most S. cerevisiae telomeres have expressed genes

To determine the expression state of all genes at all 32 *S. cerevisiae* telomeres, we performed mRNA-Seq on RNA samples from WT and *sir2Δ*, *sir3Δ*, and *sir4Δ* strains. The *MAT* locus, which specifies mating type, was deleted in these strains to allow nearly complete, unambiguous read mapping between the two silent-mating-type cassettes *HMLα* and *HMRa*. Analysis of mRNAs in WT and *sir2Δ* strains across all subtelomeric regions revealed several important generalizations (Figure 4 and Figure S5; the highly similar results for *sir3Δ* and *sir4Δ* are shown in Figure S6 and Figure S7). All chromosomes had numerous genes within 20 kbp of the ends that were expressed. Transcription occurred within 5 kbp of most ends. Thus there was no evidence supporting widespread Sir-based repression of most genes near telomeres. For most of the transcripts detected in subtelomeric regions, there was no detectable increase in transcript number in *sir2Δ* relative to WT strains. For some loci, transcription increased modestly in *sir2Δ* strains (ORFs shown in red; genes listed in Table 1). An important and expected exception was *HMLα1* and *HMLα2*; these genes showed a substantial increase in expression in *sir2Δ* strains (see *TEL03L* 15 kbp from end). Interestingly, repression at *TEL03L* extended approximately 12 kbp beyond *HMLα* to the end of chromosome III because all annotated ORFs in this region increased in expression in *sir2Δ* strains (Table 1). Sir2 was found to be enriched across this entire domain as well, along with hypoacetylated H4K16. Thus the expression status in WT strains correlated with these two marks of heterochromatin. This was the only telomere for which

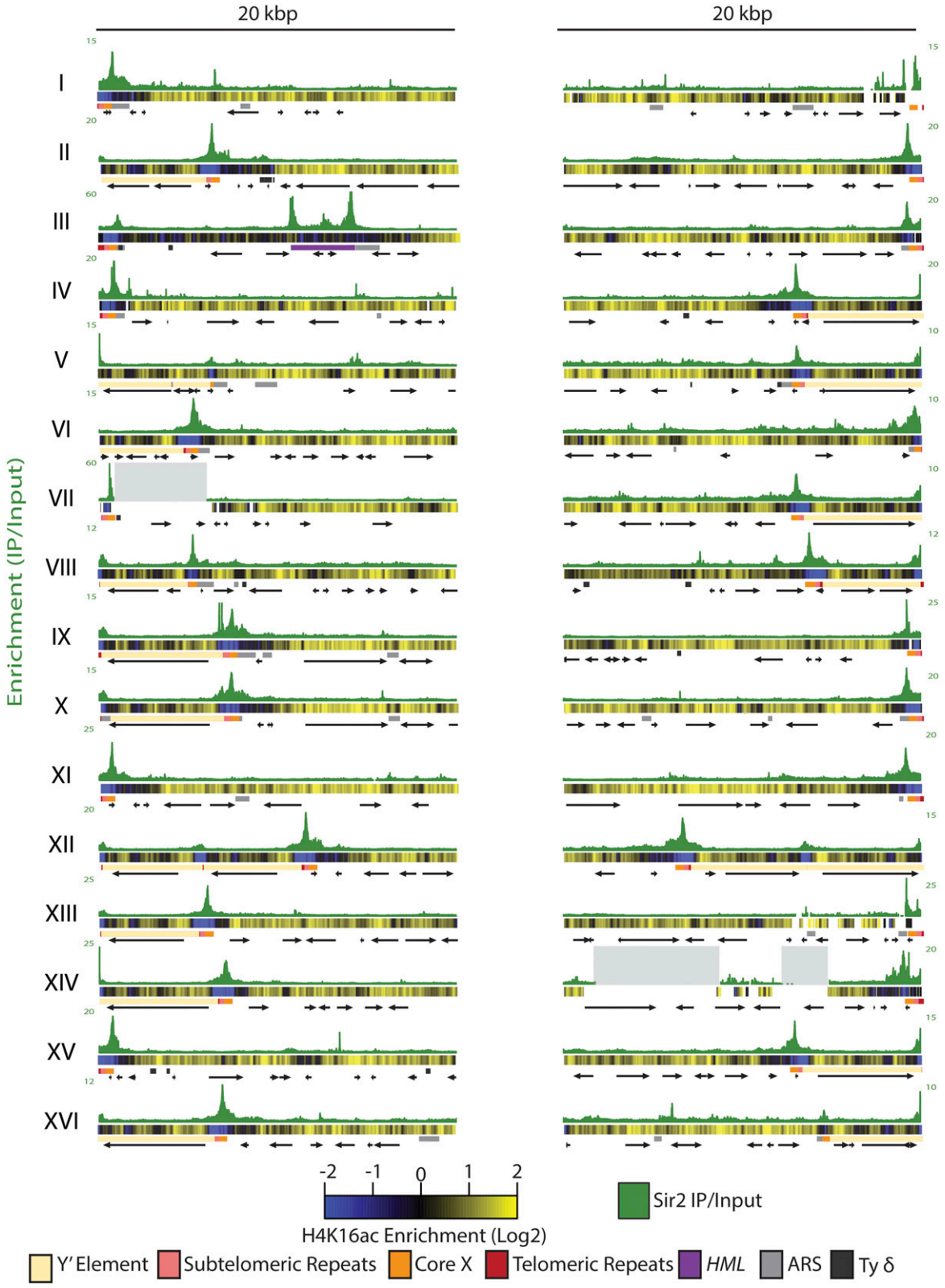

Figure 2 H4K16 exhibited hypoacetylation in regions greater than Sir2 protein association. Sir2 enrichment is shown for each telomere as the IP/input for that base-pair position. Below the Sir2 enrichment track for each telomere is a heat map representing the $\log_2$ of H4K16 IP/input. Blue represents regions of hypoacetylation where the IP value is below the input value, and yellow represents IP/input values greater than 1, which indicate acetylated regions. Salient features for each telomere are shown: telomeric repeats as red boxes, subtelomeric repeats as pink boxes, the core X as orange boxes, and *HML* as a dark-purple rectangle. Origins of replication and Ty δ elements are marked in light gray and dark gray, respectively. ORFs are represented by black arrows. All features were mapped as annotated in the SGD.

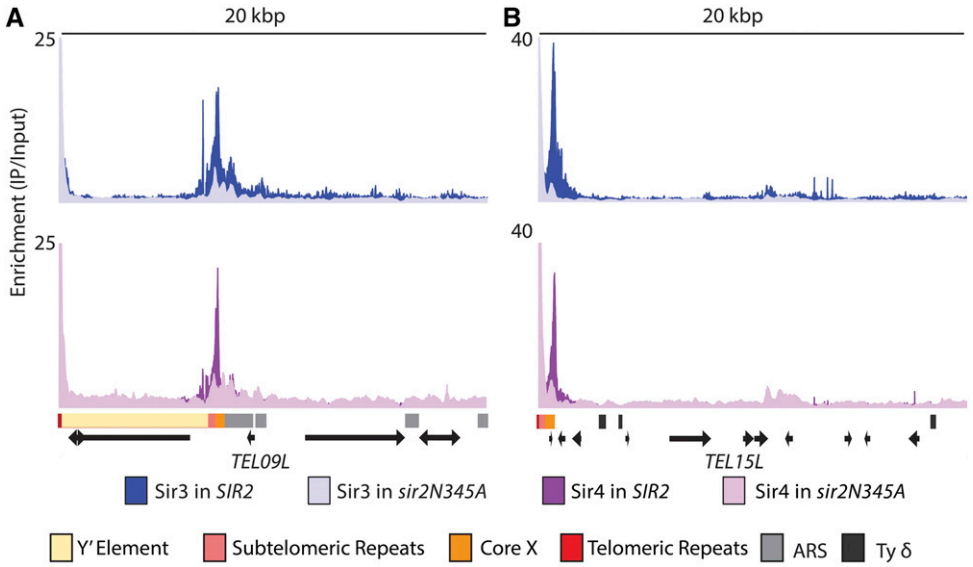

Figure 3 Sir3 and Sir4 association in strains lacking Sir2 catalytic activity. ChIP-Seq reads of Myc-tagged Sir3 and Sir4 in a strain expressing a catalytically inactive point mutant *SIR2* allele, *SIR2N345A*, were analyzed at the telomeres. A representative X-Y′ telomere is shown in A, and a representative X-only telomere is shown in B. The upper panel shows Sir3 association in the WT *SIR2* strain (dark blue) and the mutant *sir2N345A* background (light blue). The lower panel shows Sir4 association in the WT *SIR2* strain (dark purple) and the mutant *sir2N345A* background (light purple). Salient features for each telomere are as in Figure 2.

there was evidence of a Sir protein–mediated domain of repression.

Telomeres produced significantly fewer transcripts than nontelomeric loci

Once we observed transcription at subtelomeric domains, we wanted to determine how transcription at telomeres and subtelomeric domains compared to transcription at nontelomeric loci. Though transcripts were detected from many of the genes at subtelomeric regions, these genes had lower expression levels (FPKM values) on average than nontelomeric genes. We compared the distribution of FPKM values of subtelomeric protein-coding genes to non-subtelomeric protein-coding genes and found a statistically significant lower level of FPKM values among subtelomeric genes (Figure 5). These data corroborate previous subtelomeric transcript quantification in *S. cerevisiae* (Wyrick *et al.* 1999; Teytelman *et al.* 2008). This decreased transcription at telomeres could be attributed, in part, to decreased ORF density at telomeres (Louis 1995).

Only ~6% of subtelomeric genes were silenced by Sir proteins

To determine the extent to which Sir proteins affect the expression of subtelomeric genes, we performed a differential gene expression analysis using the DESeq package in R (Anders and Huber 2013). Genes showing a statistically significant difference in expression from WT (as indicated by a P-value < 0.05), a greater than twofold change in expression, and a false discovery rate of less than 10% (to control for the multiple-testing problem) were included in the final list of differentially expressed genes. Using these criteria, 42 genes appeared to be up-regulated in all three *sir* mutants (for a complete list of all statistically significant observed expression changes, see Table S7). In principle, these 42 genes were expected to fall into either of two categories: (1) genes directly subject to Sir-based repression (*e.g.*, genes at *HMLα*, *HMRa*, and subtelomeric regions) and (2) genes normally expressed more highly in a/α diploids as a result of simultaneous *HML* and *HMR* de-repression in *sir* mutants. Of these 42 genes, 21 (50%) were in subtelomeric regions (Table 1 and Figure 4, red arrows). Of these, 13 were completely repressed or averaged less that 1 FPKM among replicate experiments in WT strains. However, even in *sir* mutant conditions, many of these genes had low expression levels, averaging at ~3.8 FPKM (Table 1). The remaining genes were expressed from two- to sixfold higher in *sir* mutants than in WT strains, with some highly expressed even in WT strains (*e.g.*, *CHA1* and *HXK1*). A previous study found *BNA1* to increase in *sir2Δ* strains (Bernstein *et al.* 2000); our data did not reproduce this finding.

For the 21 subtelomeric genes that were up-regulated in all three *sir* mutants, we evaluated whether proximity to Sir proteins influenced repression. First, we determined whether the genes that increased expression in all three mutants were within peaks as defined by MACS. Most (15 of 21) of the genes whose expression changes in all three *sir* mutants (Table 1) were within MACS peaks (Table S1). For 17 of these up-regulated genes, the distance between the midpoint of the gene and the midpoint of the nearest prominent Sir protein peak was less than 2 kbp (Table 1, last column). Four such examples of Sir-repressed coding genes adjacent to Sir peaks are shown in Figure 6. Another gene, *COS6*, displayed a significantly enriched peak for only Sir4, and the expression of this gene increased ~1.4-fold relative to WT in the *sir4Δ* strain (because it did not increase in *sir2Δ* and *sir3Δ* strains, this gene is not included in Table 1). Proximity to a Sir protein peak was not, however, predictive of whether or not a gene would be de-repressed in a *sir* mutant. There were many genes that either fell under a Sir protein peak or fell within 2 kbp of a Sir protein peak

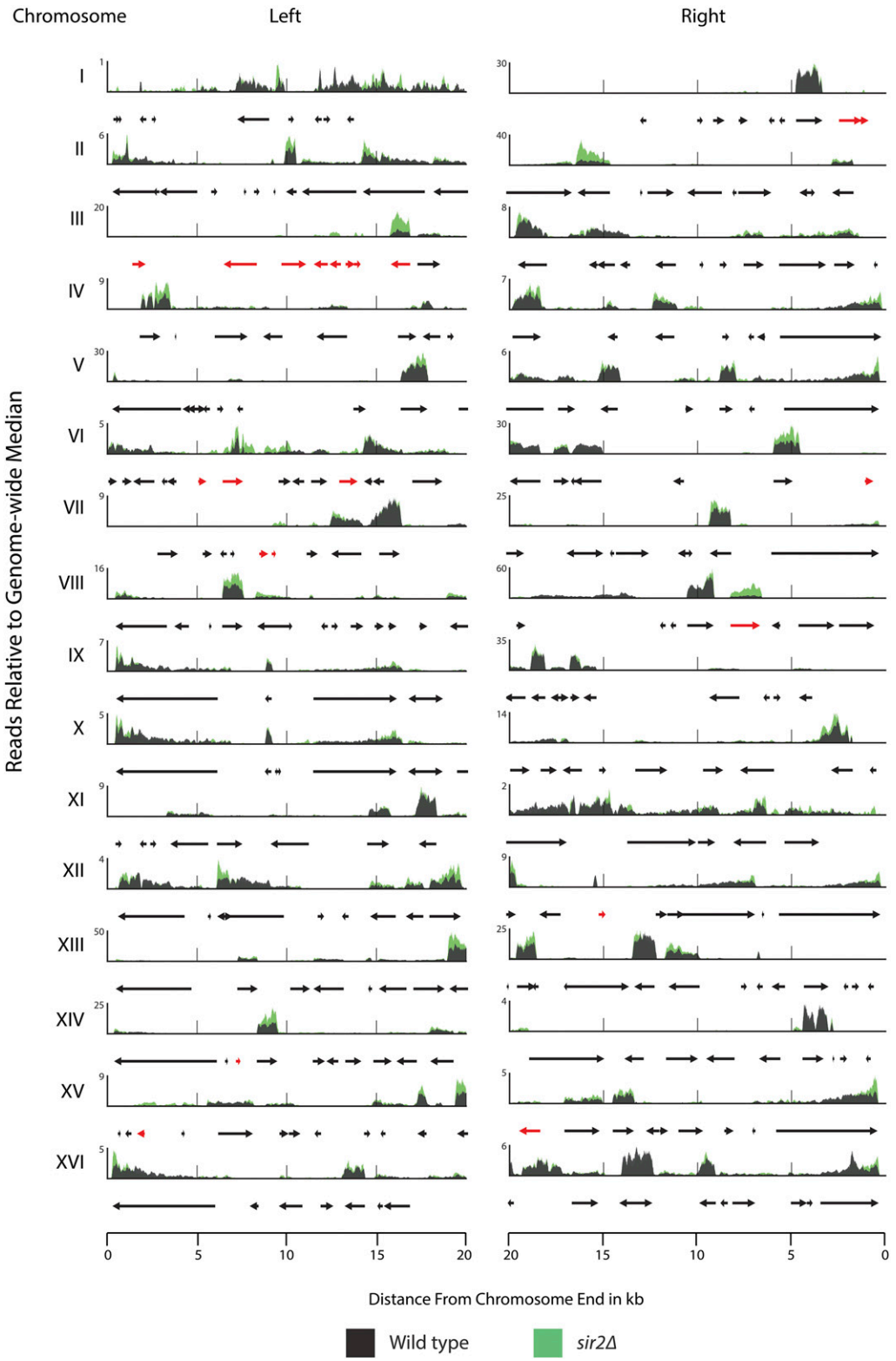

Figure 4 Transcription at all 32 telomeres in WT and *sir2Δ* strains. RNA-Seq was performed on WT and *sir2Δ* strains. Shown are read pileups from WT (black) and *sir2Δ* (green). Read pileups are normalized to the median genome-wide coverage and are the average of three biological replicates. Genes that showed a twofold or greater increase in expression in all three *sir* mutants (*sir2Δ*, *sir3Δ*, and *sir4Δ*) are colored as red arrows. Genes that showed no significant change in expression between WT and all three *sir* mutants are in black.

but did not change in expression in a *sir* mutant. Of the 101 coding genes that fell within 2 kbp of Sir2 peaks, 84 (~83%) were not de-repressed in a *sir2Δ* strain. Additionally, there were three genes that MACS called as significantly enriched for at least one of the three Sir proteins but whose expression did not change in the sir mutants: *IRC7*, *VBA5*, and *PAU20*. *PAU20* was previously implicated as a secondary recruitment site for Sir3 (Radman-Livaja *et al.* 2011). Thus Sir proteins can be recruited to a loci without repressing the adjacent gene.

Table 1 Subtelomeric genes under Sir2/3/4 repression

Gene	Systematic name	Wild type	*sir2Δ*	*sir3Δ*	*sir4Δ*	Distance to nearest sir peak (bp)
IMD1	*YAR073W*	0.1	1.1	1.1	1.1	1,575
YAR075W	*YAR075W*	1.6	26	21.9	25	846
YCL076W	*YCL076W*	0	3.3	2.8	3.5	0
YCL075W	*YCL075W*	0	1.9	2.6	2.8	0
YCL074W	*YCL074W*	0	4.5	6.5	4.9	0
GEX1	*YCL073C*	0.1	0.4	0.5	0.5	0
VBA3	*YCL069W*	0.4	3.5	3.9	4.5	0
YCL068C	*YCL068C*	0.1	4.8	0.5	7.4	0
YCL065W	*YCL065W*	0	14.9	9.1	9.2	0
CHA1	*YCL064C*	51.2	148	229.4	242.2	0
YFL063W	*YFL063W*	0	1.7	1.2	0.4	175
COS4	*YFL062W*	5	12.5	15.3	18.1	1,527
THI5	*YFL058W*	1.3	4.4	3.8	3.1	7,972
YFR057W	*YFR057W*	0.2	12	9.7	10.8	529
YPS5	*YGL259W*	0.2	2.9	3.3	2.7	2,836
YGL258W-A	*YGL258W-A*	3.4	13.1	27.8	29.7	3,396
IMD2	*YHR216W*	61.5	234.2	331.9	352.5	989
PAU4	*YLR461W*	0.5	1.1	1.6	1.9	1,239
YNL337W	*YNL337W*	0	2.2	0.4	0.6	77
AAD15	*YOL165C*	2.1	7.2	10.1	10.4	0
FDH1	*YOR388C*	1.4	2.7	2.5	2.7	11,622

Shown in this table are the expression values in FPKM for the 21 subtelomeric genes that increased in expression in *sir2Δ*, *sir3Δ*, and *sir4Δ*. Genes are ordered by chromosome number and map position. FPKM values represent the average of three biological replicates. Distances to nearest Sir peaks were calculated by taking the difference of the midpoint of the gene and the genomic coordinate of the highest nearby Sir protein IP/input enrichment value.

At least 13 Y′ elements were expressed

There are 19 annotated Y′ elements, all near the telomeres in the S288C genome. A small percentage (0.010–0.058%) of the total reads in each RNA-Seq library mapped to Y′ elements (Table S3), corroborating previous work on the expression of Y′ elements (Pryde and Louis 1999). The high degree of sequence similarity among Y′ elements precluded microarray experiments from being able to determine which of the Y′ elements were expressed. Likewise, most of our reads from Y′ elements (~81%) did not map uniquely to specific Y′ elements. Using the ~19% that mapped uniquely due to SNPs that distinguish Y′ elements (read counts shown in Table S4), we found that 13 Y′ elements were expressed. Absolute differences in read counts were difficult to interpret because the number of uniquely mapped reads per Y′ element varies as a function of the number of unique SNPs within its sequence. Nevertheless, in no case was the level of expression significantly higher or lower in a *sir* mutant relative to WT strains (Table S4). Six Y′ elements (*TEL04R-YP*, *TEL16L-YP*, *TEL07R-YP*, *TEL12R-YP1*, *TEL14L-YP*, and *TEL15R-YP*) contributed no uniquely mapped reads.

Others have detected telomere-repeat-containing RNAs (TERRAs) originating from the repeated sequences within X elements (Iglesias *et al.* 2011). We detected a small percentage of sequence reads that mapped to sufficiently polymorphic X elements and found that X elements present at *TEL02L*, *TEL06L*, *TEL06R*, *TEL07R*, and *TEL11R* increased in expression in all three *sir* mutants. However, the transcripts we detected originated from the core X, which contains the Abf1 and ORC binding sites, not the repeats within X elements.

Newly identified haploid- or diploid-regulated genes

S. cerevisiae cell type is specified by the activity of transcription factors encoded by alleles of the *MAT* locus [reviewed in Haber (2012)]. These transcription factors activate or repress transcriptional programs in each of the three cell types. Haploid yeast mutants for *SIR2*, *SIR3*, or *SIR4* simultaneously express the α2 and a1 proteins as a result of derepression of *HMLα* and *HMRa*, respectively. Dimerization of a1 and α2 leads to the a1/α2 repressor complex, which represses haploid-specific genes by directly binding to their promoters. α2 also dimerizes with Mcm1 and represses a-specific genes. Our data provided an opportunity to use the enhanced resolving power and sensitivity of RNA-Seq to obtain a potentially full catalog of haploid-specific genes and a/α-specific genes. Therefore, any previously undiscovered a-specific genes also may be included among the haploid-specific genes because of their decreased expression in *sir* mutants relative to WT strains.

We applied the following criteria to obtain a list of candidate cell-type-specific genes: (1) the gene increased or decreased in all three *sir* mutants compared to WT strains, (2) the gene's expression level had a twofold or greater statistically significant change, and (3) the gene was not directly bound by Sir2, Sir3, or Sir4. Using these criteria, we identified 16 genes with elevated expression in *sir* mutants (Table 2). Six of these genes have mitochondrial functions (*FMP43*, *SFC1*, *CYC7*, *CYC1*, *NCA3*, and *YJL133C-A*) and are clearly expressed in haploids as well. Hence these genes were more accurately interpreted as having a/α-enhanced expression. No common functions were found for the remaining 11 genes, nor have any diploid functions been

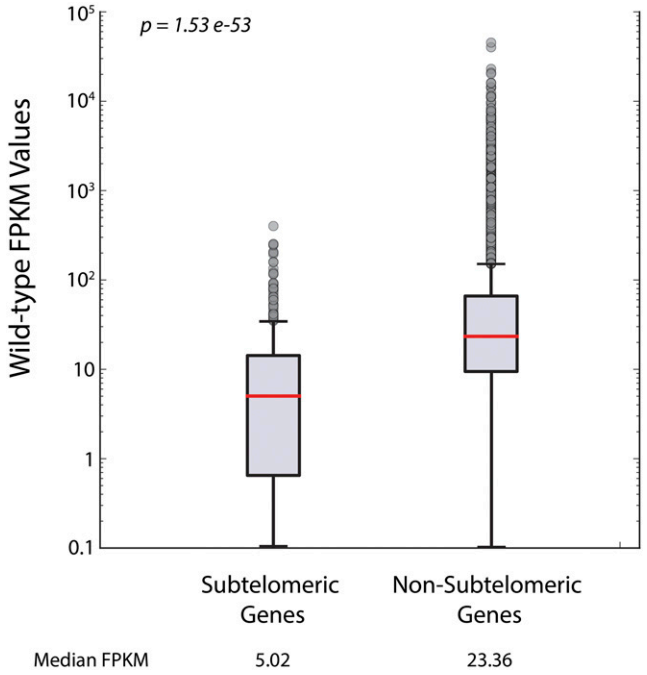

Figure 5 FPKM values for subtelomeric genes were significantly lower than FPKM values for non-subtelomeric genes. The distribution in FPKM values of subtelomeric genes was compared to the distribution of FPKM values of non-subtelomeric genes in the WT genetic background using the Wilcoxon rank-sum test. The median FPKM value for subtelomeric genes was 5.02, whereas the median FPKM value for non-subtelomeric genes was 23.4 (*P*-value = 1.53^{-53}).

attributed to these. To evaluate the dependence of these expression changes on the presence of the a1/α2 dimer, *HMLα* was deleted in the *sir2Δ* background, and expression changes were measured using qRT-PCR. The expression increase for *YJL133C-A* depended on the presence of α2 (Figure 7C), making it a candidate for indirect regulation by a1/α2 (perhaps through *RME1*, for example).

Thirty-five genes decreased in expression in *sir* mutants relative to WT strains. We compared this list to known haploid-specific genes as found by chromatin immunoprecipitation of α2 in a/α diploids followed by hybridization of immunoprecipitated DNA to a genome-wide array (Galgoczy *et al.* 2004). That study found 20 haploid-specific genes, all of which were reproduced in our data set (Table 2, genes without footnote markers). *YGL193C* and the anti-sense transcript of *IME4*, which are positioned in tandem, are also known a1/α2 targets that were reproduced in our data set (Hongay *et al.* 2006; Valencia-Burton *et al.* 2006). An additional known indirect a1/α2 target reproduced in our data set was the G1 cyclin gene *CLN2*. *CLN2* is weakly activated by *RME1* and therefore, as expected, decreased in expression in *sir* mutants presumably because of the repression of *RME1* itself (Table 2) (Toone *et al.* 1995).

The remaining 13 of 35 genes in the decreasing-genes list represented genes with previously unrecognized haploid-specific or a-specific expression (Table 2, genes with footnote markers). To further evaluate whether these genes were direct targets of a1/α2 or α2/Mcm1 repression, we performed two additional tests: (1) a scan of each gene's promoter sequences for the presence of annotated a1/α2 or α2/Mcm1 binding motifs using the motif discovery program MEME and the *Ye*ast *T*ranscription *Fa*ctor *S*pecificity *Co*mpendium (YeTFaSpCo) (Bailey *et al.* 2009; De Boer and Hughes 2012) and (2) measurement of the expression of each gene via qRT-PCR in a *sir2Δ hmlΔ* strain. If the observed expression change were in fact due to the presence of a1/α2, deleting α2 should abolish the effect. For both tests, known a1/α2 and α2/Mcm1 targets served as positive controls. Four genes with previously unrecognized haploid-specific expression were confirmed with these two tests: *STE14*, *TOS1*, *AXL2*, and *MHF2*. Interestingly, none of the four were under strong a1/α2 repression. Instead, they appeared to be weakly repressed by α2 (Figure 7A). Consistent with this observation, none possessed clear a1/α2 binding motifs of the kind found in the strongly repressed haploid-specific genes *STE2* and *HO*. However, weak a1/α2 or α2 binding sites, as annotated in the YeTFaSpCo, were found for all four (Figure 7B).

Discussion

This study provided a comprehensive evaluation of both the molecular topology of Sir protein distribution at telomeres and subtelomeric regions and of the extent of telomere position effects on gene expression mediated by Sir-based gene silencing. The *URA3* reporter gene and other reporter genes near truncated telomeres have served as an assay for telomere position effects for many years. Their use has enabled multiple discoveries, including the gene for the RNA component of telomerase (Singer and Gottschling 1994), and has implicated many chromatin factors and histone modifications as key players in silencing genes near telomeres. However, because repression of the *URA3* reporter at the truncated telomere of *TEL07L* is robust, there exists a commonly held view that all natural telomeres of *S. cerevisiae* are transcriptionally silent and that most, if not all, subtelomeric genes are strongly repressed by the Sir protein complex. By measuring expression at native telomeres using the highly sensitive RNA-Seq method, we found that many genes near telomeres are transcribed, albeit at lower levels than the rest of the genome, supporting and extending earlier data that expression of genes in subtelomeric regions of *S. cerevisiae* is largely uninfluenced by Sir proteins (Takahashi *et al.* 2011). Moreover, we found that Sir-based silencing was not a widespread phenomenon at telomeres despite strong enrichment of Sir proteins at telomeric repeats and core X elements. Twenty-one genes in the vicinity of Sir proteins are de-repressed, but most genes are not, resulting in only 6% of subtelomeric genes repressed by Sir proteins. Qualitatively, these data are in agreement with a high-density microarray-based genome-wide expression study of WT strains and *sir2Δ*, *sir3Δ*, and *sir4Δ* mutants (Wyrick *et al.* 1999).

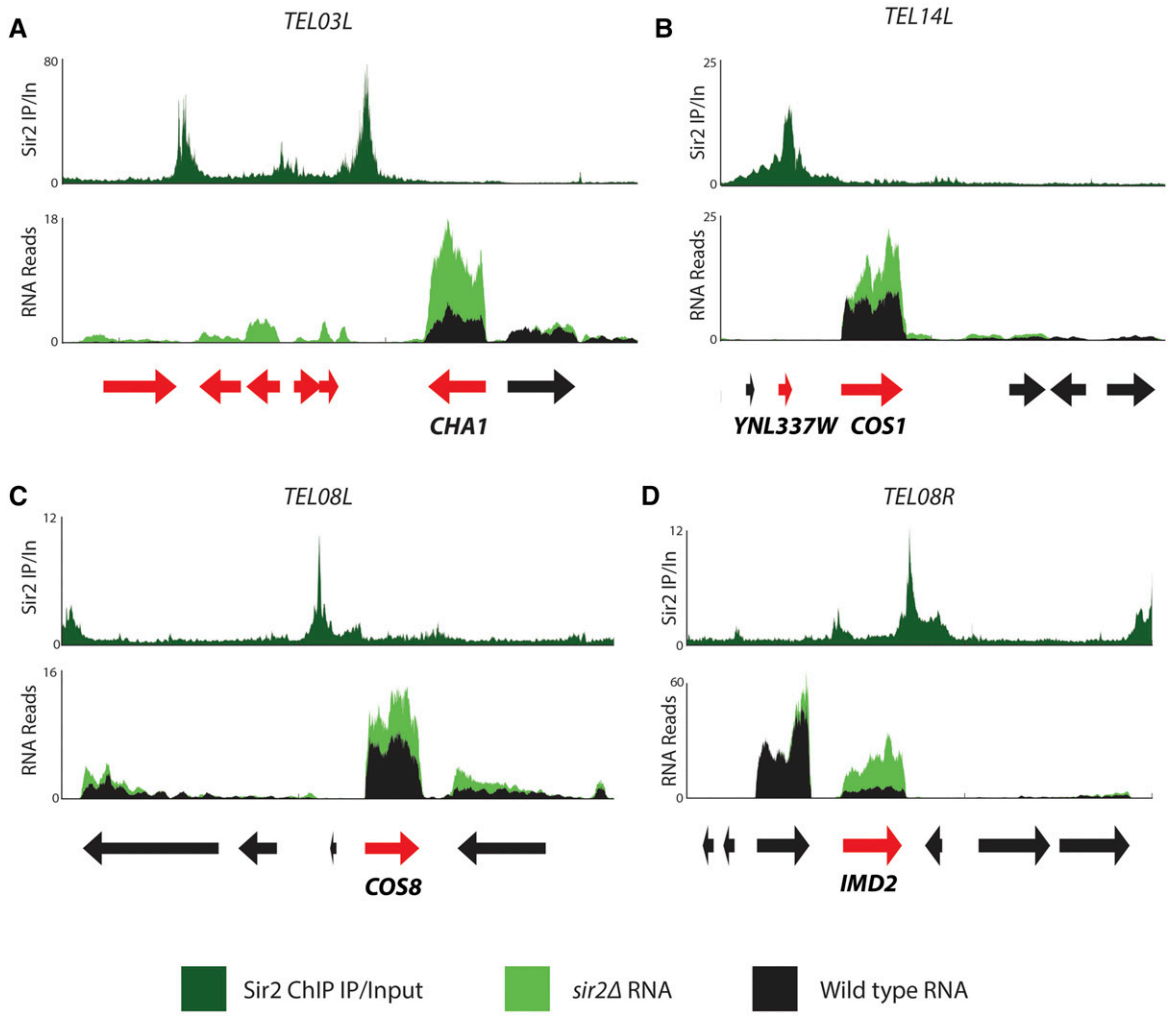

Figure 6 Genes that were de-repressed in *sir* mutants tended to be located near peaks of Sir binding. For each panel, the top horizontal axis shows Sir2 ChIP IP/input. The lower panel shows expression in the form of RNA read pileups in WT (black) and *sir2Δ* (green) strains. Genes that showed a statistically significant increase in expression in *sir2Δ* relative to WT are colored in red. (A) Left arm of chromosome III, *TEL03L*. *CHA1* is adjacent to a peak of Sir2 present at the *HML E* silencer. (B) Left arm of chromosome XIV, *TEL14L*. Both *YNL337W* and *COS1* are adjacent to a peak of Sir2 and were de-repressed in the *sir2Δ* mutant. (C and D) Left and right arms of chromosome VIII, *TEL08L* and *TEL08R*, respectively. Both *COS8* and *IMD2* are adjacent to a peak of Sir2 and showed increased expression in the *sir2Δ* mutant.

Transcription occurs near telomeres but at lower levels than at nontelomeric regions

Although transcription does occur in subtelomeric regions, it produces fewer transcripts per gene than nontelomeric regions of the genome. This global observation is consistent with previous studies that found telomeres to be both gene-poor and, for the genes present, to have lower levels of transcription than is typical for the rest of the genome, as measured by hybridization studies with high-density microarrays (Louis 1995; Wyrick *et al.* 1999). A limitation of all RNA-based studies to date is their reliance on mRNA samples from a large population of cells. Hence high-level expression in a small fraction of cells but no expression in most would have been missed. Indeed, the epigenetic inheritance of expression states observed for reporter genes at telomeres underscores the existence of such cell-to-cell variation.

Importantly, however, transcript levels at subtelomeric regions in *sir* mutants did not match transcript levels from non-subtelomeric regions. Therefore, Sir protein binding at telomeres was not solely responsible for the low transcript levels from most genes in subtelomeric regions. Other factors potentially responsible for the lower expression of subtelomeric genes include (1) other non–Sir protein chromatin factors that might confer an additional tier of repression on subtelomeric genes and (2) sequence-specific reasons for low subtelomeric expression, such as the use of intrinsically weak promoters. In support of the first possibility, histone H4 depletion increases expression of 15% of subtelomeric genes, whereas *sir* mutations increase expression of only

Table 2 Mating-type regulated genes

Gene	Systematic name	Wild type	*sir2Δ*	*sir3Δ*	*sir4Δ*
Genes increasing in expression					
YJL047C-A[a]	*YJL047C-A*	0	39.2	9.5	11.8
YER053C-A[a]	*YER053C-A*	0	777.5	1640.7	371.2
SFC1[a]	*YJR095W*	0.8	1.6	1.4	1.8
FMP43[a]	*YGR243W*	1.3	10.4	8.5	8.3
JID1[a]	*YPR061C*	3.2	9.1	8.3	8.5
GTO3[a]	*YMR251W*	3.7	7.6	8.5	10.6
YDR042C[a]	*YDR042C*	4.6	19.4	14.6	10.7
HMX1	*YLR205C*	6.7	29.3	44	24.5
MTH1[a]	*YDR277C*	6.8	14.3	18.8	16.6
YKR075C[a]	*YKR075C*	8.1	24.6	36.1	38.5
NCA3[a]	*YJL116C*	10.1	24.4	28.4	25.8
YJR115W[a]	*YJR115W*	11.2	20.9	21.3	24.5
CYC7[a]	*YEL039C*	11.2	26.8	99.7	62.9
YDR119W-A[a]	*YDR119W-A*	27	70.8	145.3	136.2
YJL133C-A[a]	*YJL133C-A*	67.2	183.8	152	303.5
CYC1[a]	*YJR048W*	130.8	444.2	513.5	267.8
AHP1[a]	*YLR109W*	218.2	480.6	438.6	526.6
Genes decreasing in expression					
SNO3[a]	*YFL060C*	7.8	2	2.4	3.1
HUA2[a]	*YOR284W*	10	3.8	4.3	4.6
HO	*YDL227C*	10.7	1.7	0.8	1.1
AXL1	*YPR122W*	15	4.3	3.6	2.9
STE5	*YDR103W*	15.1	1.7	2.7	2.3
YPR027C[a]	*YPR027C*	16.1	2.7	3.5	4.1
YDR170W-A	*YDR170W-A*	16.1	3.9	4.6	3.5
SST2[a]	*YLR452C*	16.8	7	7.5	6.5
RDH54	*YBR073W*	16.9	3.3	3.7	2.7
NEJ1	*YLR265C*	19	2.4	2.1	1.6
YDR034C-D[a]	*YDR034C-D*	25.8	6.1	15.4	12
STE6	*YKL209C*	25.9	2.9	4.1	3.6
GPA1	*YHR005C*	26.1	3.5	2.8	2.8
ICS2	*YBR157C*	31.4	5.8	4.6	5.1
VBA2[a]	*YBR293W*	35.1	8.2	10	8
BAR1	*YIL015W*	44.7	4.3	3.2	3.2
FUS3	*YBL016W*	49.1	1.1	0.8	0.9
MHF2[a]	*YDL160C-A*	49.7	19.9	13.5	18.6
AXL2[a]	*YIL140W*	49.7	14.8	21.8	14.9
CLN2[a]	*YPL256C*	50.3	21.9	20.6	19.6
IME4	*YGL192W*	53.8	6	8	7.4
STE14[a]	*YDR410C*	75.6	23.5	21.5	17
STE4	*YOR212W*	75.8	8	7.3	5.8
YGL193C	*YGL193C*	79.2	2.6	3.3	4.2
STE18	*YJR086W*	82.8	10.8	10.7	5.3
AGA2	*YGL032C*	87.8	0.5	2	2.3
DDR2	*YOL052C-A*	97.3	39.2	41.2	29.8
AMN1	*YBR158W*	102.5	39.4	39.5	33.6
RME1	*YGR044C*	108.2	5.1	6.7	4.8
MFA1	*YDR461W*	227.3	0	0	0
SUN4[a]	*YNL066W*	311.4	125.2	122.1	136.1
STE2	*YFL026W*	327.7	5.5	5.5	5.8
ZRT1[a]	*YGL255W*	389.9	110.8	117.2	160.9
TOS1[a]	*YBR162C*	1143.3	437.3	557.7	478.5
MFA2[b]	*YNL145W*	3465.9	0	71.6	0

All genes in this table (1) changed significantly in expression in all three *sir* mutants relative to WT and (2) are *not* located at *HML*, *HMR*, or subtelomeric regions. Seventeen genes increased in expression, and 35 decreased in expression.

[a] Genes not found in previous lists of haploid-specific or haploid-enhanced genes Expression levels are in units of FPKM, and genes are ordered by increasing FPKM levels in WT.

[b] The FPKM value for *MFA2* in the *sir3Δ* strain, though greater than 0, is not statistically different from the value of 0 FPKM seen in *sir2Δ* and *sir4Δ* strains. Similar numbers of raw reads mapped to the *MFA2* locus in all three mutants (18, 19, and 11 average reads for *sir2Δ*, *sir3Δ*, and *sir4Δ*, respectively). The inflated FPKM value seen in the *sir3Δ* strain is likely a consequence of the FPKM normalization method used by Cufflinks, which, because of the substantially larger library size of the *sir3Δ* strains (Table S2), may have overestimated the FPKM value for the lowly expressed *MFA2* gene.

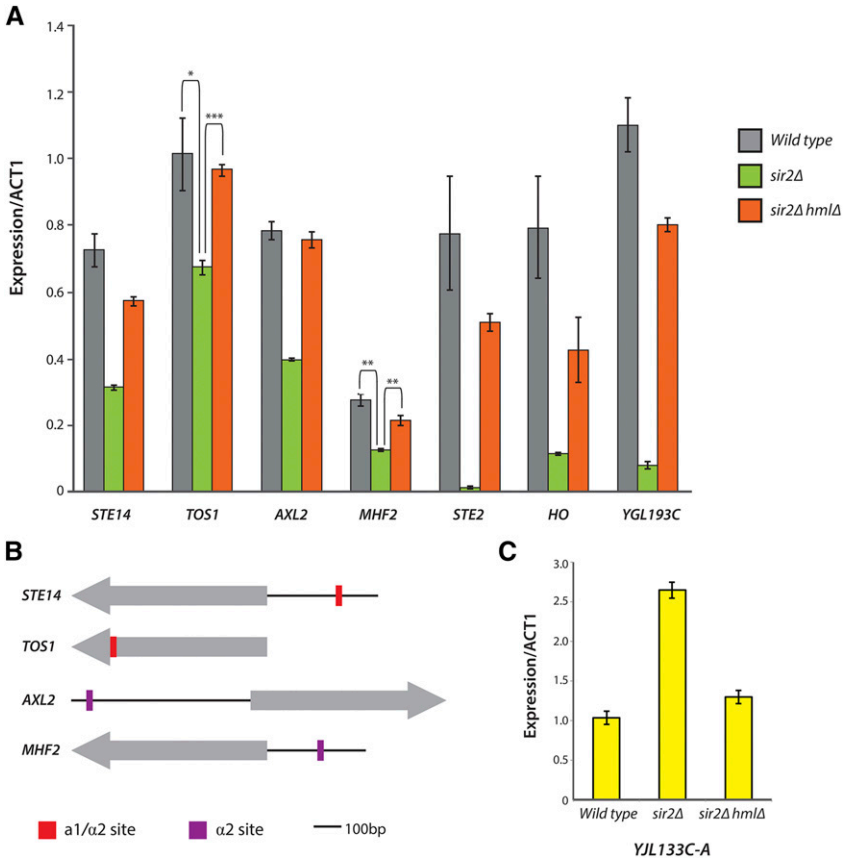

Figure 7 Expression confirmation via qRT-PCR and promoter analysis of candidate haploid-specific genes. (A) *STE14*, *TOS1*, *AXL2*, and *MHF2* were weakly repressed in an α2-dependent manner. The strongly a1/α2-repressed genes *STE2*, *HO*, and *YGL193C* are shown for comparison. (B) Annotated binding sites for the a1/α2 heterodimer and α2 itself are shown in relation to the protein-coding sequences (gray arrows) for *STE14*, *TOS1*, *AXL2*, and *MHF2* (coding regions are not drawn to scale). *STE14* contains a weak a1/α2 binding site 232 bp upstream from its coding sequence. *TOS1* contains a weak a1/α2 binding site within its gene body. Both *AXL2* and *MHF2* contain weak α2 binding sites 578 and 174 bp, respectively, upstream from their coding regions. (C) *YJL133C-A*, a gene of unknown function, increases in expression in a α2-dependent manner.

7–9% of genes within subtelomeric regions (Wyrick *et al.* 1999; Martin *et al.* 2004). Our data show that a similar percentage (~6%) of subtelomeric genes are repressed by Sir proteins. Perhaps other chromatin factors targeting histone H4 confer an additional repressive effect on subtelomeric regions. Silencing at different telomeres also might be more or less sensitive to distinct histone-modifying enzymes. For example, the subtelomeric gene *FLO10*, which encodes a cell wall glycoprotein, is repressed by the action of deacetylases Hst1 and Hst2, two paralogs of Sir2 (Halme *et al.* 2004). Additionally, there is almost no agreement as to the identity of the genes repressed by Dot1 (Takahashi *et al.* 2011), the enzyme that catalyzes H3K79 methylation, and those repressed by *SIR2* (this study), which deacetylates H4K16-acetyl.

The second possible reason that subtelomeric domains exhibit lower levels of transcription could be that subtelomeric genes, on average, have weaker promoters than centromere-proximal genes. If subtelomeric genes tend to have weaker promoters and lack transcriptional activator binding sites, it would be expected that most are weakly expressed regardless of chromatin state. Interestingly, subtelomeric genes are among the most highly divergent genes in the yeast genome and are often up-regulated under stressful conditions (Harrison *et al.* 2002; Teytelman *et al.* 2008). Previous studies have shown that part of the reason for this elevated rate of divergence is the ability of Sir proteins to interfere with certain types of DNA repair, highlighting a functional consequence of Sir protein association (Terleth *et al.* 1989). Our data implied that this mechanism could not account for all the enhanced divergence in these regions because the distribution of Sir proteins was focal rather than throughout the region. However, given that some mechanisms of DNA repair are transcription coupled (Svejstrup 2002), perhaps the low expression level of genes (or cell-to-cell variation in expression) in the subtelomeric regions leads to the absence of transcription-coupled repair and thereby contributes to their rapid divergence. If so, the higher mutation rate could, in turn, result in reduced functioning of promoter elements. Furthermore, a higher proportion of ORFs at telomeres are categorized as "dubious" or "uncharacterized," with ~56% of subtelomeric genes falling into these two categories as opposed to ~24% of non-subtelomeric genes. Thus many subtelomeric ORFs may not be functional protein-coding genes whose expression is needed for general cellular function.

Only a small fraction of subtelomeric genes were repressed by Sir proteins

Overall, we found that Sir proteins repressed only 6% of all subtelomeric genes. Why are some subtelomeric genes repressed by Sir proteins and others not? Certain strong transcription activators can efficiently escape Sir-based repression (D. Steakley and J. Rine, unpublished results). Perhaps genes with increased expression in the absence of Sir proteins possess promoters with binding sites for weak

transcriptional activators or weak binding sites for strong activators. In the absence of Sir proteins, these weakly binding activators would gain access and promote transcription. If so, the promoters of these Sir protein–sensitive genes might contain transcription factor binding sites that are distinct from binding sites present at genes that are not repressed by Sir proteins. To explore this possibility, we cataloged the transcription factor binding profiles for the promoters of the 21 *SIR*-sensitive subtelomeric genes and compared them to each other as well as to the transcription factor binding profiles from all other subtelomeric genes. Overall, we found no differences in transcription factor binding profiles between *SIR*-sensitive and *SIR*-resistant subtelomeric genes, though the small number of genes involved limited any statistical power of the analysis (data not shown). Motifs for the Mot2 and Ash1 transcription factors were the most commonly found sequences in the data set for all subtelomeric genes analyzed regardless of whether they were Sir repressed or not. Furthermore, 13 of the 21 *SIR*-sensitive genes are annotated as "dubious," and the remaining 8 shared no common functional annotations, consistent with an absence of common transcription factor binding sites. In sum, we were unable to find differences in promoter sequence or transcription factor binding sites between the genes that were repressed by Sir proteins and those that were not.

The functional significance of Sir proteins at telomeres

At present, one clear function of Sir proteins at telomeres is to repress, or at least lower, the expression of a small subset of genes in this part of the genome. But why would a cell want to simply lower the expression of genes in this way, as opposed to simply having a weaker promoter for such genes? Perhaps subtelomeric genes regulated by Sir proteins in *S. cereivisiae*, like those in *C. glabrata* (De Las Peñas *et al.* 2003; Domergue *et al.* 2005; Ma *et al.* 2009), are involved in regulating the transcription of genes that are necessary only under certain conditions. In support of this model, seven genes encoding metabolic enzymes increased in expression in all three *sir* mutants: *CHA1*, *AAD15*, *IMD2*, *FDH1*, *THI5*, *VBA3*, and *PAU4*. It is possible that *S. cerevisiae* encounters some condition in nature that would inhibit Sir-based silencing like nicotinamide does in the laboratory. If so, perhaps these enzymes are part of an as yet undiscovered response mechanism to such agents or conditions.

A second hypothesis is that Sir proteins at telomeres contribute to the suppression of recombination at telomeric repeats, much like Sir2 suppresses recombination at the recombinant DNA repeats (Gottlieb and Esposito 1989; Smith and Boeke 1997). While yeast Ku proteins, which associate with Sir proteins at the subtelomeric core X sequences, do suppress recombination between telomeric repeats (Marvin *et al.* 2009), so far there is no direct evidence that Sir proteins are involved in this suppression. Additionally, a previous observation that Sir proteins associate with Ku70/Ku80 (suggesting a role for Sir proteins in preventing nonhomologous end joining), as reported by Tsukamoto *et al.* (1997), has since been shown to be an artifact of the a/α state of *sir* mutants (Åström *et al.* 1999).

Discovery of novel haploid-specific genes

Historically, elucidation of transcriptional regulatory circuits of *S. cerevisiae* has relied on microarray-based technologies, which are limited in sensitivity and dynamic range (Galgoczy *et al.* 2004). The sensitivity of RNA-Seq and the "pseudo-diploid" state of *sir* mutants allowed us to evaluate the completeness of the identification of cell-type-regulated genes, particularly genes that are potential targets of a1/α2 and α2/Mcm1 regulation. We confirmed all previously identified genes of these classes. In addition, we found 29 new candidate haploid-specific or a/α-specific genes. Of these 29 genes, the expression of *YJL133C-A*, *STE14*, *TOS1*, *AXL2*, and *MHF2* was verified by qRT-PCR and found to be moderately repressed in an α2-dependent manner, thus revealing a new class of genes that are partially but not fully repressed in the a/α cell type. The remaining 24 genes were too low in expression to be verified by qRT-PCR. The cell-type regulation of these genes was likely missed in previous studies precisely because they are not strongly repressed and thus exhibit a less dramatic fold change in expression than other a/α-regulated genes. At least three of the five genes were verified by qRT-PCR function in processes unrelated to cell-type determination. For example, *STE14* encodes a methyltransferase that methylates a-factor in *MAT***a** cells and Ras proteins in all cell types (Marr *et al.* 1990; Hrycyna *et al*. 1991). On a per-cell basis, it is likely that more a-factor is produced in *MAT***a** cells than Ras proteins in all cell types, consistent with the partial reduction in *STE14* expression in cells that do not make a-factor because of the expression of α2. We speculate that the Tos1, Mhf2, and Axl1 proteins have functions needed in all cell types, leading to their modest repression in a/α diploids.

Acknowledgments

We thank Minyong Chung and the Vincent J. Coates Genomics Sequencing Laboratory at the University of California, Berkeley, supported by National Institutes of Health S10 Instrumentation grants S10-RR029668 and S10-RR027303. This work was supported by a grant from the National Institutes of Health (GM-31105 to J.R.), National Science Foundation Predoctoral Fellowships (to A.E. and D.T.), a Berkeley Fellowship to A.E., and the University of California, Berkeley's Cellular, Biochemical and Molecular Training Grant T32 GM 007127 from the National Institutes of Health.

Literature Cited

Ai, W., P. G. Bertram, C. K. Tsang, T. Chan, and X. F. S. Zheng, 2002 Regulation of subtelomeric silencing during stress response. Mol. Cell 10: 1295–1305.

Anders, S., and W. Huber, 2010 Differential expression analysis for sequence count data. Genome Biol. 11: R106.

Anders S., and W. Huber, 2013 Differential expression of RNA-Seq data at the gene level: the DESeq package. Available at: http://www.bioconductor.org/packages/devel/bioc/vignettes/DESeq/inst/doc/DESeq.pdf Accessed: March 1, 2014.

Aparicio, O. M., B. L. Billington, and D. E. Gottschling, 1991 Modifiers of position effect are shared between telomeric and silent mating-type loci in S. cerevisiae. Cell 66: 1279–1287.

Åström, S. U., S. M. Okamura, and J. Rine, 1999 Yeast cell-type regulation of DNA repair. Nature 397: 310.

Bailey, T. L., M. Boden, F. A. Buske, M. Frith, C. E. Grant *et al.*, 2009 MEME SUITE: tools for motif discovery and searching. Nucleic Acids Res. 37: W202–W208.

Bernstein, B. E., J. K. Tong, and S. L. Schreiber, 2000 Genomewide studies of histone deacetylase function in yeast. Proc. Natl. Acad. Sci. USA 97: 13708–13713.

de Boer, C. G., and T. R. Hughes, 2012 YeTFaSCo: a database of evaluated yeast transcription factor sequence specificities. Nucleic Acids Res. 40: D169–D179.

Collart, M. A., and S. Oliviero, 2001 Preparation of yeast RNA, pp. 13.12.1–13.12.5 in *Current Protocols in Molecular Biology*, Wiley, Hoboken, NJ.

Crampton, A., F. Chang, D. L. J. Pappas, R. L. Frisch, and M. Weinreich, 2008 An ARS element inhibits DNA replication through a SIR2-dependent mechanism. Mol. Cell 30: 156–166.

De Las Peñas, A., S. Pan, I. Castaño, J. Alder, R Cregg *et al.*, 2003 Virulence-related surface glycoproteins in the yeast pathogen *Candida glabrata* are encoded in subtelomeric clusters and subject to RAP1- and SIR-dependent transcriptional silencing. Genes Dev. 17: 2245–2258.

Domergue, R., I. Castan, A. De Las Peñas, M. Zupancic, V. Lockatell *et al.*, 2005 Nicotinic acid limitation regulates silencing of Candida adhesins during UTI. Science 308: 866–870.

Ehrentraut, S., J. M. Weber, J. N. Dybowski, D. Hoffmann, and A. E. Ehrenhofer-Murray, 2010 Rpd3-dependent boundary formation at telomeres by removal of Sir2 substrate. Proc. Natl. Acad. Sci. USA 107: 5522–5527.

Fourel, G., E. Revardel, C. E. Koering, and É. Gilson, 1999 Cohabitation of insulators and silencing elements in yeast subtelomeric regions. EMBO J. 18: 2522–2537.

Galgoczy, D. J., A. Cassidy-Stone, M. Llinas, S. M. O'Rourke, I. Herskowitz *et al.*, 2004 Genomic dissection of the cell-type-specification circuit in Saccharomyces cerevisiae. Proc. Natl. Acad. Sci. USA 101: 18069–18074.

Gottlieb, S., and R. E. Esposito, 1989 A new role for a yeast transcriptional silencer gene, *SIR2*, in regulation of recombination in ribosomal DNA. Cell 56: 771–776.

Gottschling, D. E., O. M. Aparicio, B. L. Billington, and V. A. Zakian, 1990 Position effect at *S. cerevisiae* telomeres: reversible repression of Pol II transcription. Cell 63: 751–762.

Guizetti, J., and A. Scherf, 2013 Silence, activate, poise and switch! Mechanisms of antigenic variation in *Plasmodium falciparum*. Cell. Microbiol. 15: 718–726.

Haber, J. E., 2012 Mating-type genes and *MAT* switching in *Saccharomyces cerevisiae*. Genetics 191: 33–64.

Halme, A., S. Bumgarner, C. Styles, and G. R. Fink, 2004 Genetic and epigenetic regulation of the *FLO* gene family generates cell-surface variation in yeast. Cell 116: 405–415.

Harrison, P., A. Kumar, N. Lan, N. Echols, M. Snyder *et al.*, 2002 A small reservoir of disabled ORFs in the yeast genome and its implications for the dynamics of proteome evolution. J. Mol. Biol. 316: 409–419.

Hazelrigg, T., R. Levis, and G. M. Rubin, 1984 Transformation of white locus DNA in *Drosophila*: dosage compensation, zeste interaction, and position effects. Cell 36: 469–481.

Hecht, A., S. Strahl-Bolsinger, and M. Grunstein, 1996 Spreading of transcriptional repressor SIR3 from telomeric heterochromatin. Nature 383: 92–96.

Hongay, C. F., P. L. Grisafi, T. Galitski, and G. R. Fink, 2006 Antisense transcription controls cell fate in *Saccharomyces cerevisiae*. Cell 127: 735–745.

Hoppe, G. J., J. C. Tanny, A. D. Rudner, S. A. Gerber, S. Danaie *et al.*, 2002 Steps in assembly of silent chromatin in yeast: Sir3-independent binding of a Sir2/Sir4 complex to silencers and role for Sir2-dependent deacetylation. Mol. Cell. Biol. 22: 4167–4180.

Hrycyna, C. A., S. K. Sapperstein, S. Clarke, and S. Michaelis, 1991 The Saccharomyces cerevisiae STE14 gene encodes a methyltransferase that mediates C-terminal methylation of a-factor and RAS proteins. *The* EMBO Journal, 10(5): 1699–1709.

Iglesias, N., S. Redon, V. Pfeiffer, M. Dees, J. Lingner *et al.*, 2011 Subtelomeric repetitive elements determine TERRA regulation by Rap1/Rif and Rap1/Sir complexes in yeast. EMBO Rep. 12: 587–593.

Kurdistani, S. K., D. Robyr, S. Tavazoie, and M. Grunstein, 2002 Genome-wide binding map of the histone deacetylase Rpd3 in yeast. Nat. Genet. 31: 248–254.

Li, H., and R. Durbin, 2009 Fast and accurate short read alignment with Burrows-Wheeler transform. Bioinformatics 25: 1754–1760.

Li, H., B. Handsaker, A. Wysoker, T. Fennell, J. Ruan *et al.*, 2009 The sequence alignment/map format and SAMtools. Bioinformatics 25: 2078–2079.

Li, M., V. Valsakumar, K. Poorey, S. Bekiranov, and J. S. Smith, 2013 Genome-wide analysis of functional sirtuin chromatin targets in yeast. Genome Biol. 14: R48.

Loney, E. R., P. W. Inglis, S. Sharp, F. E. Pryde, N. A. Kent *et al.*, 2009 Repressive and non-repressive chromatin at native telomeres in *Saccharomyces cerevisiae*. Epigenet. Chromatin 2: 18.

Longtine, M. S., A. McKenzie, III, D. J. Demarini, N. G. Shah, A. Wach *et al.*, 1998 Additional modules for versatile and economical PCR-based gene deletion and modification in *Saccharomyces cerevisiae*. Yeast 14: 953–961.

Louis, E. J., 1995 The chromosome ends of *Saccharomyces cerevisiae*. Yeast 11: 1553–1573.

Ma, B., S.-J. Pan, R. Domergue, T. Rigby, M. Whiteway *et al.*, 2009 High-affinity transporters for NAD^+ precursors in *Candida glabrata* are regulated by Hst1 and induced in response to niacin limitation. Mol. Cell. Biol. 29: 4067–4079.

Marr, R. S., L. C. Blair, and J. Thorner, 1990 Saccharomyces cerevisiae STE14 gene is required for COOH-terminal methylation of a-factor mating pheromone. J. Biol. Chem. 265(33): 20057–20060.

Martin, A. M., D. J. Pouchnik, J. L. Walker, and J. J. Wyrick, 2004 Redundant roles for histone H3 N-terminal lysine residues in subtelomeric gene repression in *Saccharomyces cerevisiae*. Genetics 167: 1123–1132.

Marvin, M. E., M. M. Becker, P. Noel, S. Hardy, A. A. Bertuch *et al.*, 2009 The association of yKu with subtelomeric core X sequences prevents recombination involving telomeric sequences. Genetics 183: 453–467.

Pappas, D. L. J., R. Frisch, and M. Weinreich, 2004 The NAD (+)-dependent Sir2p histone deacetylase is a negative regulator of chromosomal DNA replication. Genes Dev. 18: 769–781.

Pryde, F. E., and E. J. Louis, 1999 Limitations of silencing at native yeast telomeres. EMBO J. 18: 2538–2550.

Radman-Livaja, M., G. Ruben, A. Weiner, N. Friedman, R. Kamakaka *et al.*, 2011 Dynamics of Sir3 spreading in budding yeast: secondary recruitment sites and euchromatic localization. EMBO J. 30: 1012–1026.

Renauld, H., O. M. Aparicio, P. D. Zierath, B. L. Billington, S. K. Chhablani *et al.*, 1993 Silent domains are assembled continuously

from the telomere and are defined by promoter distance and strength, and by SIR3 dosage. Genes Dev. 7: 1133–1145.
Rossmann, M. P., W. Luo, O. Tsaponina, A. Chabes, and B. Stillman, 2011 A common telomeric gene silencing assay is affected by nucleotide metabolism. Mol. Cell 42: 127–136.
Rusche, L. N., A. L. Kirchmaier, and J. Rine, 2002 Ordered nucleation and spreading of silenced chromatin in *Saccharomyces cerevisiae*. Mol. Biol. Cell 13: 2207–2222.
Schultz, J., 1947 The nature of heterochromatin. Cold Spring Harb. Symp. Quant. Biol. 12: 179–191.
Singer, M. S., and D. E. Gottschling, 1994 TLC1: template RNA component of *Saccharomyces cerevisiae* telomerase. Science 266: 404–409.
Smith, J. S., and J. D. Boeke, 1997 An unusual form of transcriptional silencing in yeast ribosomal DNA. Genes Dev. 11: 241–254.
Strahl-Bolsinger, S., A. Hecht, K. Luo, and M. Grunstein, 1997 SIR2 and SIR4 interactions differ in core and extended telomeric heterochromatin in yeast. Genes Dev. 11: 83–93.
Svejstrup, J. Q., 2002 Mechanisms of transcription-coupled DNA repair. Nat. Rev. Mol. Cell Biol. 3: 21–29.
Takahashi, Y.-H., J. M. Schulze, J. Jackson, T. Hentrich, C. Seidel *et al.*, 2011 Dot1 and histone H3K79 methylation in natural telomeric and HM silencing. Mol. Cell 42: 118–126.
Terleth, C., C. A. van Sluis, and P. van de Putte, 1989 Differential repair of UV damage in *Saccharomyces cerevisiae*. Nucleic Acids Res. 17: 4433–4439.
Teytelman, L., M. B. Eisen, and J. Rine, 2008 Silent but not static: accelerated base-pair substitution in silenced chromatin of budding yeasts. *PLoS Genet.* 4: e1000247.
Teytelman, L., D. M. Thurtle, J. Rine, A. Oudenaarden, and van, 2013 Highly expressed loci are vulnerable to misleading ChIP localization of multiple unrelated proteins. Proc. Nat. Acad. Sci. USA 110: 18602–18607.
Thurtle, D. M., and J. Rine, 2014 The molecular topography of silenced chromatin in *Saccharomyces cerevisiae*. Genes Dev. 28: 245–258.
Tonkin, C. J., C. K. Carret, M. T. Duraisingh, T. S. Voss, S. A. Ralph *et al.*, 2009 Sir2 paralogues cooperate to regulate virulence genes and antigenic variation in *Plasmodium falciparum*. PLoS Biol. 7: e1000084.
Toone, W. M., A. L. Johnson, G. R. Banks, J. H. Toyn, D. Stuart *et al.*, 1995 Rmel, a negative regulator of meiosis, is also a positive activator of G1 cyclin gene expression. EMBO J. 14: 5824–5832
Trapnell, C., L. Pachter, and S. L. Salzberg, 2009 TopHat: discovering splice junctions with RNA-Seq. Bioinformatics 25: 1105–1111.
Trapnell, C., A. Roberts, L. Goff, G. Pertea, D. Kim *et al.*, 2012 Differential gene and transcript expression analysis of RNA-seq experiments with TopHat and Cufflinks. Nat. Protoc. 7: 562–578.
Tsukamoto, Y., J. Kato, and H. Ikeda, 1997 Silencing factors participate in DNA repair and recombination in Saccharomyces cerevisiae. Nature 388: 900–903.
Valencia-Burton, M., M. Oki, J. Johnson, T. A. Seier, R. Kamakaka *et al.*, 2006 Different mating-type-regulated genes affect the DNA repair defects of *Saccharomyces RAD51*, *RAD52* and *RAD55* mutants. Genetics 174: 41–55.
Wellinger, R. J., and V. A. Zakian, 2012 Everything you ever wanted to know about *Saccharomyces cerevisiae* telomeres: beginning to end. Genetics 191: 1073–1105.
Wyrick, J. J., F. C. P. Holstege, E. G. Jennings, H. C. Causton, D. Shore *et al.*, 1999 Chromosomal landscape of nucleosome-dependent gene expression and silencing in yeast. Nature 402: 418–421.
Yoshida, K., J. Bacal, D. Desmarais, I. Padioleau, O. Tsaponina *et al.*, 2014 The histone deacetylases Sir2 and Rpd3 act on ribosomal DNA to control the replication program in budding yeast. Mol. Cell 54: 691–697.
Zhang, Y., T. Liu, C. A. Meyer, J. Eeckhoute, D. S. Johnson *et al.*, 2008 Model-based analysis of ChIP-Seq (MACS). Genome Biol. 9: R137.
Zhu, X., and C. M. Gustafsson, 2009 Distinct differences in chromatin structure at subtelomeric X and Y′ elements in budding yeast. PLoS ONE 4: e6363.
Zill, O. A., D. Scannell, L. Teytelman, and J. Rine, 2010 Co-evolution of transcriptional silencing proteins and the DNA elements specifying their assembly. *PLoS Biol.* 8: e1000550.

Communicating editor: A. Gasch

GENETICS

Supporting Information
www.genetics.org/lookup/suppl/doi:10.1534/genetics.115.175711/-/DC1

The Chromatin and Transcriptional Landscape of Native *Saccharomyces cerevisiae* Telomeres and Subtelomeric Domains

Aisha Ellahi, Deborah M. Thurtle, and Jasper Rine

DOI: 10.1534/genetics.115.175711

TABLE S1 ChIP-Seq Peaks Called with MACS

MACS was used to call peaks of significant enrichment for the Sir protein ChIP-Seq datasets. The "Sir" column indicates the Sir protein dataset (either Sir2, Sir3 or Sir4) that the peak was identified in. The start and end coordinates indicate the chromosomal coordinate of the peak as identified by MACS. A "yes" in columns 5-7 indicate that the peak was detected in that dataset for the particular Sir protein and a "No" indicates that the peak was not called in that dataset. The "Genome Features" column indicates the genome features within the starting and ending coordinates of the peak as annotated in SGD.

Sir	Telomere	start	end	Sonication Replicate 1	Sonication Replicate 2	MNase	Genome Features
Sir2	*TEL01-L*	1	3165	Yes	Yes	Yes	TR, X element, *PAU8*
Sir3	*TEL01-L*	1	3204	Yes	Yes	Yes	TR, X element, *PAU8*
Sir4	*TEL01-L*	1	3211	Yes	Yes	Yes	TR, X element, *PAU8*
Sir2	*TEL01-L*	1	1905	No	Yes	Yes	Y'
Sir3	*TEL02-L*	1	8824	No	Yes	Yes	X-Y', *PAU9*
Sir4	*TEL02-L*	1	8824	Yes	Yes	Yes	X-Y', *PAU9*
Sir2	*TEL02-L*	4924	8824	Yes	Yes	Yes	X element, *PAU9*
Sir2	*TEL03-L*	1	18568	Yes	Yes	Yes	TR, X element, *YCL076W, YCL075W, YCL074W, GEX1, VBA3, YCL068C, YCL065W, HML, CHA1*
Sir3	*TEL03-L*	1	18622	Yes	Yes	Yes	TR, X element, *YCL076W, YCL075W, YCL074W, GEX1, VBA3, YCL068C, YCL065W, HML, CHA1*
Sir4	*TEL03-L*	1	15202	Yes	Yes	Yes	TR, X element, *YCL076W, YCL075W, YCL074W, GEX1, VBA3, YCL068C, YCL065W, HML*
Sir4	*TEL03-L*	15460	18178	Yes	Yes	Yes	*HML*
Sir4	*TEL03-R*	312518	315021	Yes	Yes	Yes	TR, X element
Sir2	*TEL03-R*	313064	315102	Yes	Yes	Yes	TR, X element
Sir2	*TEL04-L*	1	1725	Yes	Yes	Yes	TR, X element
Sir3	*TEL04-L*	1	1800	Yes	Yes	Yes	TR, X element
Sir4	*TEL04-L*	1	1731	Yes	Yes	Yes	TR, X element
Sir4	*TEL04-R*	1521508	1525877	No	Yes	Yes	X element, *PAU10*
Sir3	*TEL04-R*	1522260	1526289	Yes	Yes	Yes	X element, *PAU10*
Sir2	*TEL04-R*	1522281	1526268	Yes	Yes	Yes	X element, *PAU10*

Sir3	*TEL04-R*	1526513	1529507	No	Yes	Yes	Y'
Sir2	*TEL09-L*	1	5882	Yes	Yes	Yes	Y'
Sir3	*TEL09-L*	1	5999	Yes	Yes	Yes	Y'
Sir4	*TEL09-L*	1	7027	Yes	Yes	Yes	Y'
Sir2	*TEL09-L*	6054	9980	Yes	Yes	Yes	X element, *PAU14*
Sir3	*TEL09-L*	6057	10087	Yes	Yes	Yes	X element, *PAU14*
Sir4	*TEL09-L*	7049	9980	Yes	Yes	Yes	X element, *PAU14*
Sir4	*TEL09-L*	16947	18692	No	Yes	Yes	IMA3
Sir4	*TEL09-R*	437481	439152	No	Yes	Yes	X element
Sir2	*TEL09-R*	437501	439339	No	Yes	Yes	X element
Sir2	*TEL05-L*	1	7618	Yes	Yes	Yes	X-Y'
Sir3	*TEL05-L*	1	7804	Yes	Yes	Yes	X-Y'
Sir4	*TEL05-L*	1	7826	Yes	No	Yes	X-Y'
Sir4	*TEL05-R*	567524	571291	No	Yes	Yes	X element
Sir2	*TEL05-R*	568755	571249	No	Yes	Yes	X element
Sir3	*TEL05-R*	568818	571793	No	Yes	Yes	X element
Sir4	*TEL06-L*	1	7113	Yes	Yes	Yes	X-Y', *YFL063W, COS4, YFL058W*
Sir3	*TEL06-L*	1	7067	No	Yes	Yes	X-Y', *YFL063W, COS4, YFL058W*
Sir2	*TEL06-L*	374	8410	No	Yes	Yes	X-Y', *YFL063W, COS4, YFL058W*
Sir4	*TEL06-R*	263978	265355	Yes	Yes	No	*IRC7*
Sir3	*TEL06-R*	263993	265339	Yes	Yes	Yes	*IRC7*
Sir2	*TEL06-R*	264026	265321	Yes	No	Yes	*IRC7*
Sir3	*TEL07-L*	1	875	Yes	Yes	No	TR, X-element
Sir4	*TEL07-R*	1081144	1083523	No	Yes	Yes	*COS6*
Sir2	*TEL07-R*	1082655	1085210	Yes	Yes	Yes	X element
Sir3	*TEL07-R*	1083258	1085832	No	Yes	Yes	X element
Sir3	*TEL07-R*	1085851	1087178	No	Yes	Yes	Y'
Sir2	*TEL08-L*	1	2478	Yes	Yes	Yes	X element
Sir3	*TEL08-L*	1	2476	Yes	Yes	Yes	X element
Sir4	*TEL08-L*	1	6631	Yes	Yes	Yes	X-Y'
Sir3	*TEL08-L*	4505	6572	No	Yes	Yes	X element
Sir2	*TEL08-L*	4521	6542	Yes	Yes	Yes	X element
Sir4	*TEL08-R*	552041	558152	Yes	Yes	No	X element, Y', *IMD2*
Sir3	*TEL08-R*	552750	562261	No	Yes	Yes	X element, Y', IMD2
Sir2	*TEL08-R*	552885	557851	Yes	Yes	Yes	X element, Y', *IMD2*
Sir2	*TEL10-L*	1	5942	Yes	Yes	Yes	Y'
Sir3	*TEL10-L*	1	7045	Yes	Yes	Yes	Y'
Sir4	*TEL10-L*	1	10006	Yes	Yes	Yes	X-Y'
Si, Y'*L10-L*	6061	9999	Yes	Yes	Yes	X element	

Sir3	*TEL10-L*	7070	10068	Yes	Yes	Yes	X element
Sir2	*TEL11-L*	1	3067	Yes	Yes	Yes	TR, X element, *PAU16*
Sir3	*TEL11-L*	1	3107	Yes	Yes	Yes	TR, X element, *PAU16*
Sir4	*TEL11-L*	1	3117	Yes	Yes	Yes	TR, X element, *PAU16*
Sir4	*TEL11-R*	658211	660866	Yes	Yes	Yes	*VBA5*
Sir3	*TEL11-R*	658212	660806	Yes	Yes	Yes	*VBA5*
Sir2	*TEL11-R*	658227	660267	Yes	Yes	Yes	*VBA5*
Sir3	*TEL11-R*	660881	663222	Yes	Yes	No	*GEX2*
Sir2	*TEL11-R*	661907	664824	X	No	Yes	*GEX2*
Sir3	*TEL12-L*	1	4543	No	Yes	Yes	Y'
Sir2	*TEL12-L*	1	4537	Yes	Yes	Yes	Y'
Sir4	*TEL12-L*	1	14200	Yes	Yes	Yes	X-Y'
Sir3	*TEL12-L*	4752	10100	Yes	Yes	Yes	X-Y'
Sir2	*TEL12-L*	4786	10091	Yes	Yes	Yes	X-Y'
Sir3	*TEL12-L*	10354	14187	No	Yes	Yes	X-Y'
Sir2	*TEL12-L*	10392	14195	Yes	Yes	Yes	X-Y'
Sir3	*TEL12-R*	1061965	1066024	No	Yes	Yes	X element, *PAU4*
Sir4	*TEL12-R*	1061988	1072866	Yes	Yes	No	X element, *PAU4*
Sir2	*TEL12-R*	1062036	1066015	Yes	Yes	Yes	X element, *PAU4*
Sir3	*TEL12-R*	1066129	1072549	No	Yes	Yes	Y'
Sir2	*TEL12-R*	1066155	1072450	Yes	Yes	Yes	Y'
Sir3	*TEL12-R*	1072672	1077188	No	Yes	Yes	Y'
Sir2	*TEL13-L*	1	4459	Yes	Yes	Yes	Y'
Sir3	*TEL13-L*	1	4429	Yes	Yes	Yes	Y'
Sir4	*TEL13-L*	1	7494	Yes	Yes	Yes	X-Y'
Sir3	*TEL13-L*	4617	7435	Yes	Yes	Yes	X element
Sir2	*TEL13-L*	4658	7401	Yes	Yes	Yes	X element
Sir2	*TEL14-L*	1	5012	Yes	Yes	Yes	Y'
Sir3	*TEL14-L*	1	5265	No	Yes	Yes	Y'
Sir4	*TEL14-L*	1	8603	Yes	Yes	Yes	X-Y'
Sir2	*TEL14-L*	5748	8491	Yes	Yes	Yes	X element
Sir3	*TEL14-L*	5748	8575	Yes	Yes	Yes	X element
Sir2	*TEL15-L*	1	2868	Yes	Yes	Yes	X element, *AAD15*
Sir4	*TEL15-L*	1	2883	Yes	Yes	Yes	X element, *AAD15*
Sir3	*TEL15-L*	1	2924	Yes	Yes	Yes	X element, *AAD15*
Sir4	*TEL15-L*	10818	12699	Yes	Yes	No	*PAU20*
Sir3	*TEL15-L*	10840	12798	Yes	Yes	No	*PAU20*
Sir3	*TEL15-R*	1082035	1085505	No	Yes	Yes	X element, *PAU21*
Sir2	*TEL15-R*	1082045	1085443	Yes	Yes	Yes	X element, *PAU21*
Sir3	*TEL15-R*	1085649	1090020	No	Yes	Yes	Y'

Sir2	*TEL16-L*	1	4519	Yes	Yes	Yes	Y'
Sir3	*TEL16-L*	1	5215	No	Yes	Yes	Y'
Sir4	*TEL16-L*	1	8760	Yes	Yes	Yes	Y'
Sir2	*TEL16-L*	5594	9094	Yes	Yes	Yes	X element
Sir3	*TEL16-L*	5648	9097	No	Yes	Yes	X element
Sir3	*TEL16-R*	941574	945387	No	Yes	Yes	X element
Sir2	*TEL16-R*	942173	944929	No	Yes	Yes	X element
Sir2	*TEL16-R*	945624	947502	No	Yes	Yes	Y'

TABLE S2 Percent Reads Mapped of RNA-Seq Data

Strain	Alias	Replicate	Total Reads	Reads Mapped	% Reads Mapped	% Mapped Non-uniquely
JRY9316	Wild type	A	15,747,860	14,480,231	92	6.94
JRY9316	Wild type	B	20,204,590	18,636,063	92	6.76
JRY9316	Wild type	C	19,988,764	18,323,263	91.7	8.98
JRY9720	*sir2Δ*	A	13,176,140	12,290,225	93	7.58
JRY9721	*sir2Δ*	B	13,865,402	12,737,081	92	6.10
JRY9722	*sir2Δ*	C	12,505,868	11,519,936	92.1	6.71
JRY9723	*sir3Δ*	A	19,925,570	18,454,658	92.6	6.8
JRY9724	*sir3Δ*	B	20,806,146	19,352,189	93	6.45
JRY9725	*sir3Δ*	C	19,655,418	18,102,386	92.1	6.43
JRY9726	*sir4Δ*	A	14,217,780	12,973,038	91	5.51
JRY9727	*sir4Δ*	B	15,272,748	14,043,542	92	6.20
JRY9728	*sir4Δ*	C	13,785,048	12,561,860	91	5.85

TABLE S3 Reads Mapped to Y' Elements

Strain	Alias	% Reads Mapped to Y'	% Of Total Y' Reads Uniquely Mapped
JRY9316	Wild type	0.044	18.8
JRY9316	Wild type	0.055	17.3
JRY9316	Wild type	0.058	18.9
JRY9720	*sir2Δ*	0.053	20.0
JRY9721	*sir2Δ*	0.056	19.9
JRY9722	*sir2Δ*	0.052	19.4
JRY9723	*sir3Δ*	0.011	19.2
JRY9724	*sir3Δ*	0.010	19.2
JRY9725	*sir3Δ*	0.010	18.7
JRY9726	*sir4Δ*	0.048	18.8
JRY9727	*sir4Δ*	0.050	18.3
JRY9728	*sir4Δ*	0.056	18.9

Average % Uniquely-Mapped Y' reads: 18.95%

TABLE S4 Normalized Read Counts Of Uniquely-Mapped Reads at Y' Elements

Y' Element	Wild type	*sir2Δ*	*sir3Δ*	*sir4Δ*
TEL04R-YP	0.0	0.0	0.0	0.0
TEL16L-YP	0.0	0.0	0.0	0.0
TEL08L-YP	130.6	185.8	159.0	174.1
TEL07R-YP	0.0	0.0	0.0	0.0
TEL06L-YP	61.8	76.6	94.3	70.9
TEL05R-YP	23.7	17.4	24.6	22.4
TEL13L-YP	3.9	3.3	5.2	5.4
TEL05L-YP	209.6	199.5	206.2	203.1
TEL12R-YP2	16.0	20.6	17.3	15.8
TEL12-R YP1	0.0	0.0	0.0	0.0
TEL14L-YP	0.0	0.0	0.0	0.0
TEL15R-YP	0.0	0.0	0.0	0.0
TEL16R-YP	78.2	61.7	53.2	56.3
TEL08R-YP	4.3	6.5	13.1	8.4
TEL10L-YP	10.5	6.2	15.3	4.8
TEL12L-YP2	16.1	15.6	13.4	20.0
TEL09L-YP	0.5	0.0	0.0	0.0
TEL02L-YP	140.5	168.3	147.4	167.7
TEL12L-YP1	0.8	0.0	0.3	0.4

TABLE S5 Strains Used In This Study

Name	Genotype	Source
JRY9316	*matΔ::HygMX can1-100 his3-11 leu2-3,112 lys2- trp1-1 ura3-52*	TEYTELMAN *et al.* 2013
JRY9720	*matΔ::HygMX can1-100 his3-11 leu2-3,112 lys2- trp1-1 ura3-52 sir2Δ::KanMX*	This study
JRY9721	*matΔ::HygMX can1-100 his3-11 leu2-3,112 lys2- trp1-1 ura3-52 sir2Δ::KanMX*	This study
JRY9722	*matΔ::HygMX can1-100 his3-11 leu2-3,112 lys2- trp1-1 ura3-52 sir2Δ::KanMX*	This study
JRY9723	*matΔ::HygMX can1-100 his3-11 leu2-3,112 lys2- trp1-1 ura3-52 sir3Δ::KanMX*	This study
JRY9724	*matΔ::HygMX can1-100 his3-11 leu2-3,112 lys2- trp1-1 ura3-52 sir3Δ::KanMX*	This study
JRY9725	*matΔ::HygMX can1-100 his3-11 leu2-3,112 lys2- trp1-1 ura3-52 sir3Δ::KanMX*	This study
JRY9726	*matΔ::HygMX can1-100 his3-11 leu2-3,112 lys2- trp1-1 ura3-52 sir4Δ::KanMX*	This study
JRY9727	*matΔ::HygMX can1-100 his3-11 leu2-3,112 lys2- trp1-1 ura3-52 sir4Δ::KanMX*	This study
JRY9728	*matΔ::HygMX can1-100 his3-11 leu2-3,112 lys2- trp1-1 ura3-52 sir4Δ::KanMX*	This study
JRY9741	*matΔ::HygMX can1-100 his3-11 leu2-3,112 lys2- trp1-1 ura3-52 sir2Δ::KanMX hmlΔ::SpHIS5MX*	This study

TABLE S6 Oligos Used in qRT-PCR Expression Analysis

Gene	Forward	Reverse
ACT1	ggcatcataccttctacaacg	ctaccggaagagtacaaggacaaaac
STE14	gaagaccaagaaggagtccg	gtagctgagtgccaattgcc
TOS1	gccaagtgacaccagcggttct	ttggccgtcatggatgtgtgag
AXL2	acggaatcactcccacaacaatgtc	ggtcttctgtctggttccatgc
MHF2	tcattgatgaggcggtgctg	cttgatgcgataactctaagggac
STE2	gataggttttatccaggcacgctg	ttgaactcgtaggtgtgggcaactg
HO	gaaatcatgtcgaggctgctg	ccatagcatctagcacatactc
YGL193C	cctttcctatagctccagcg	ccggtcacataaattgacgg

TABLE S7 Complete List of Genes Increasing in Expression in *sir2Δ, sir3Δ*, and *sir4Δ*

Shown below are expression levels in FPKM for the 107 genes that significantly increased in expression across all three *sir* mutants (*sir2Δ, sir3Δ*, and *sir4Δ*). Genes are listed in alphabetical order by gene name. Expression changes were filtered based on a p-value < 0.05 and a false-discovery rate of < 0.10. Forty-two genes (bold-faced type) showed expression changes of 2-fold or greater in *sir* mutants relative to wild type as analyzed by DESeq in terms of read counts (NOT FPKM). Transcript quantification in terms of FPKM was done with Cufflinks.

Gene	Systematic Name	Wild type	*sir2Δ*	*sir3Δ*	*sir4Δ*
AAD15	***YOL165C***	**2.1**	**7.2**	**10.1**	**10.4**
ADH7	*YCR105W*	11	15.1	15.3	15.3
ADI1	*YMR009W*	146.4	182.5	264.1	287.1
AHP1	***YLR109W***	**218.2**	**480.6**	**438.6**	**526.6**
ARO9	*YHR137W*	62.4	75.7	116.2	91.7
BNA2	*YJR078W*	7.7	11.2	14.1	12.5
BNA4	*YBL098W*	27.3	37.9	42.7	45.7
BNA5	*YLR231C*	26.8	44.2	71	69.8
CAR1	*YPL111W*	47.6	84.3	73.4	83.5
CHA1	***YCL064C***	**51.2**	**148**	**229.4**	**242.2**
CMC4	*YMR194C-B*	12.5	14.8	20.7	23.5
COA2	*YPL189C-A*	64.4	152.4	128	140.4
COS1	*YNL336W*	134	191.3	252.7	302.1
COS4	***YFL062W***	**5**	**12.5**	**15.3**	**18.1**
COS7	*YDL248W*	36	51.3	67.6	71.9
COS8	*YHL048W*	115.6	161.5	233.2	266.9
COX5A	*YNL052W*	198.4	240.4	394.7	248.9
COX6	*YHR051W*	175.9	235.6	255.3	243.4
COX7	*YMR256C*	204.3	322.7	408.4	286.6
CRC1	*YOR100C*	1.4	3.3	3.2	3.1
CYB5	*YNL111C*	146.4	254.6	572	316.5
CYC1	***YJR048W***	**130.8**	**444.2**	**513.5**	**267.8**
CYC7	***YEL039C***	**11.2**	**26.8**	**99.7**	**62.9**
CYT1	*YOR065W*	55.5	82.3	172.5	105.1
DLD1	*YDL174C*	31	40	49.8	47
EDC1	*YGL222C*	17.4	21.9	23.2	23.6
ERG13	*YML126C*	302.4	372.5	544	388
ERG6	*YML008C*	161.4	188.7	219.9	206.6
ERG8	*YMR220W*	49.2	60.6	71.6	61.8
FDH1	***YOR388C***	**1.4**	**2.7**	**2.5**	**2.7**
FMP43	***YGR243W***	**1.3**	**10.4**	**8.5**	**8.3**

GEX1	***YCL073C***	**0.1**	**0.4**	**0.5**	**0.5**
GTO3	***YMR251W***	**3.7**	**7.6**	**8.5**	**10.6**
HAP4	*YKL109W*	53.7	96.6	124.1	92.8
HMLALPHA1	***YCL066W***	**0**	**20.7**	**16.6**	**14.1**
HMLALPHA2	***YCL067C***	**0**	**38.7**	**32.3**	**48.9**
HMRA1	***YCR097W***	**0**	**40.6**	**33.4**	**39.5**
HMRA2	***YCR096C***	**0.1**	**31.9**	**23.9**	**39.5**
HMX1	***YLR205C***	**6.7**	**29.3**	**44**	**24.5**
HOR2	*YER062C*	52.9	98.8	137.2	133.8
HPF1	*YOL155C*	61.2	82.2	114.6	118.9
HSP12	*YFL014W*	51.7	126	113.8	80.1
HSP31	*YDR533C*	38.9	50.6	59.5	51.9
ICY1	*YMR195W*	97.8	209.9	154.8	175.8
IDH2	*YOR136W*	131.4	170.1	228.2	205.1
IDI1	*YPL117C*	97.6	140.3	143.1	128.8
IMD1	***YAR073W***	**0.1**	**1.1**	**1.1**	**1.1**
IMD2	***YHR216W***	**61.5**	**234.2**	**331.9**	**352.5**
JID1	***YPR061C***	**3.2**	**9.1**	**8.3**	**8.5**
MCR1	*YKL150W*	126.7	171.6	266	258.6
MET10	*YFR030W*	18.4	24.5	37.1	29.2
MET14	*YKL001C*	69.2	119	151.7	129.4
MET3	*YJR010W*	25.7	40.1	81.4	56.8
MMP1	*YLL061W*	17.1	22.8	43.6	34.9
MTH1	***YDR277C***	**6.8**	**14.3**	**18.8**	**16.6**
MVD1	*YNR043W*	202.2	242.2	333.8	252.7
NCA3	***YJL116C***	**10.1**	**24.4**	**28.4**	**25.8**
NDE1	*YMR145C*	204.4	523.2	487.4	351
NSG2	*YNL156C*	69.4	97.9	121.2	101
PAU4	***YLR461W***	**0.5**	**1.1**	**1.6**	**1.9**
PDH1	*YPR002W*	2.1	3.4	4.7	3.2
PET10	*YKR046C*	229.5	282.1	381.2	322.5
PRX1	*YBL064C*	32.5	39.7	46.3	54.7
PUT4	*YOR348C*	4.8	12.2	13.2	9.3
QCR10	*YHR001W-A*	72.4	103.2	222.3	142.1
QCR2	*YPR191W*	76.7	97.3	149.9	110.3
QCR6	*YFR033C*	149.3	247.8	247.8	233.7
QCR7	*YDR529C*	200.4	255.1	390.8	288
QCR8	*YJL166W*	193.6	289.7	396.2	318.6
QCR9	*YGR183C*	238.2	301	606	344.7
REX3	*YLR107W*	20.5	33.5	28.5	31.6
ROX1	*YPR065W*	20.5	35.1	95	57.5

RSB1	*YOR049C*	21.9	45.5	45.6	49.3
SER1	*YOR184W*	148.1	195.8	192.6	198.8
SER3	*YER081W*	102.3	135.7	131.3	160.3
SFC1	***YJR095W***	**0.8**	**1.6**	**1.4**	**1.8**
TGL2	*YDR058C*	9	12.4	13.5	15.4
THI5	***YFL058W***	**1.3**	**4.4**	**3.8**	**3.1**
UBX6	*YJL048C*	86.8	119.6	218.7	162.9
VBA3	***YCL069W***	**0.4**	**3.5**	**3.9**	**4.5**
YAR075W	***YAR075W***	**1.6**	**26**	**21.9**	**25**
YBR284W	*YBR284W*	2.1	3	3.7	4
YCL065W	***YCL065W***	**0**	**14.9**	**9.1**	**9.2**
YCL068C	***YCL068C***	**0.1**	**4.8**	**0.5**	**7.4**
YCL074W	***YCL074W***	**0**	**4.5**	**6.5**	**4.9**
YCL075W	***YCL075W***	**0**	**1.9**	**2.6**	**2.8**
YCL076W	***YCL076W***	**0**	**3.3**	**2.8**	**3.5**
YCR097W-A	*YCR097W-A*	0	8.8	5.6	6.2
YDR018C	*YDR018C*	2.2	4.2	4.1	4.5
YDR042C	***YDR042C***	**4.6**	**19.4**	**14.6**	**10.7**
YDR119W-A	***YDR119W-A***	**27**	**70.8**	**145.3**	**136.2**
YER053C-A	***YER053C-A***	**0**	**777.5**	**1640.7**	**371.2**
YFL063W	***YFL063W***	**0**	**1.7**	**1.2**	**0.4**
YFR057W	***YFR057W***	**0.2**	**12**	**9.7**	**10.8**
YGL258W-A	***YGL258W-A***	**3.4**	**13.1**	**27.8**	**29.7**
YGR182C	*YGR182C*	44.8	55.8	48.5	56.5
YIL014C-A	*YIL014C-A*	19.4	28.6	29	23.5
YJL047C-A	***YJL047C-A***	**0**	**39.2**	**9.5**	**11.8**
YJL133C-A	***YJL133C-A***	**67.2**	**183.8**	**152**	**303.5**
YJR115W	***YJR115W***	**11.2**	**20.9**	**21.3**	**24.5**
YKR075C	***YKR075C***	**8.1**	**24.6**	**36.1**	**38.5**
YLR312C	*YLR312C*	2	3.6	4.8	5.4
YLR460C	*YLR460C*	2	3.5	4.4	4.1
YMR206W	*YMR206W*	2.2	4.9	4.9	6
YNL337W	***YNL337W***	**0**	**2.2**	**0.4**	**0.6**
YNR064C	*YNR064C*	6.1	9.5	9.1	10.7
YPC1	*YBR183W*	53.8	101.6	150.1	130.5
YPS5	***YGL259W***	**0.2**	**2.9**	**3.3**	**2.7**

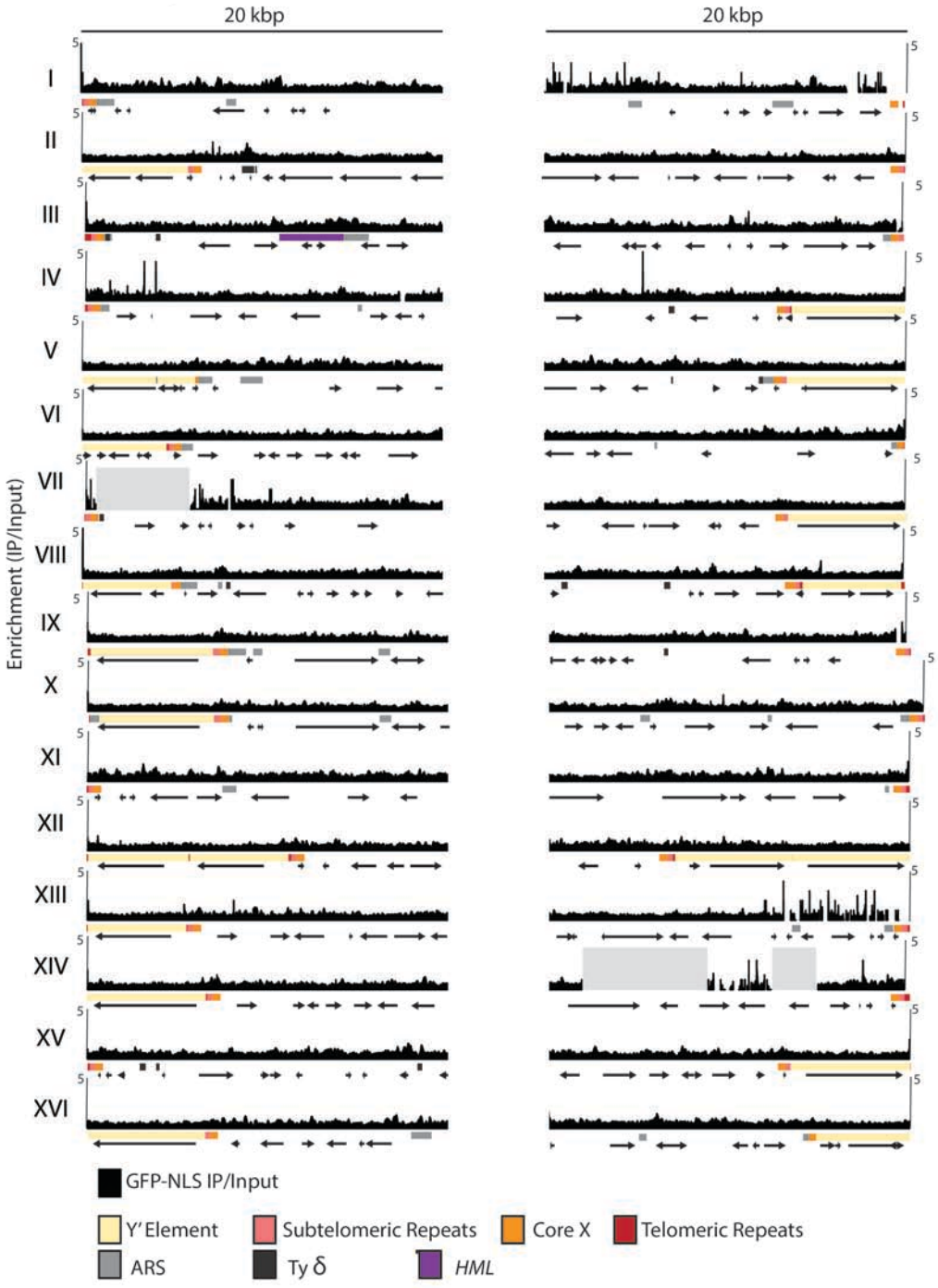

Figure S1. GFP-NLS ChIP-Seq control at all thirty-two yeast telomeres. The IP/Input enrichment values of the GFP-NLS ChIP-Seq dataset from (TEYTELMAN *et al.* 2013) was mapped at all thirty-two *S. cerevisiae* telomeres. 20 kbp for each telomere is shown. Salient features as annotated in SGD are indicated below the X-axis for each telomere as in Figure 2. The light gray rectangles indicate regions deleted in the sequenced W303 derived lab strain relative to the SGD sacCer2 reference genome.

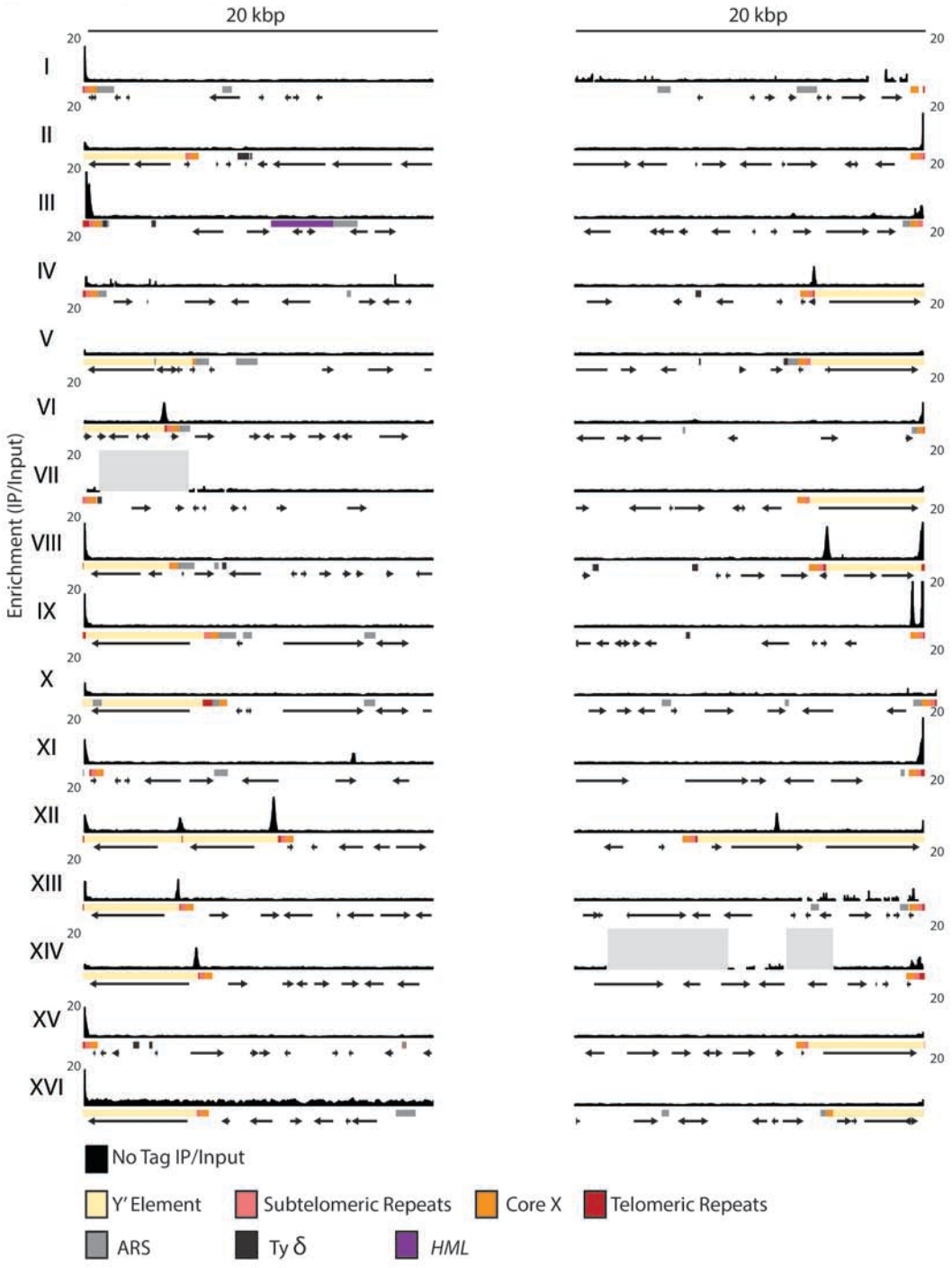

Figure S2. No tag ChIP-Seq control at all thirty-two yeast telomeres. The IP/Input enrichment values of the no tag ChIP-Seq dataset from (THURTLE and RINE 2014) was mapped at all thirty-two *S. cerevisiae* telomeres. 20 kbp for each telomere is shown. Salient features as annotated in SGD are indicated below the X-axis for each telomere as in Figure 2. The light gray rectangles indicate regions deleted in the sequenced W303 derived lab strain relative to the SGD sacCer2 reference genome.

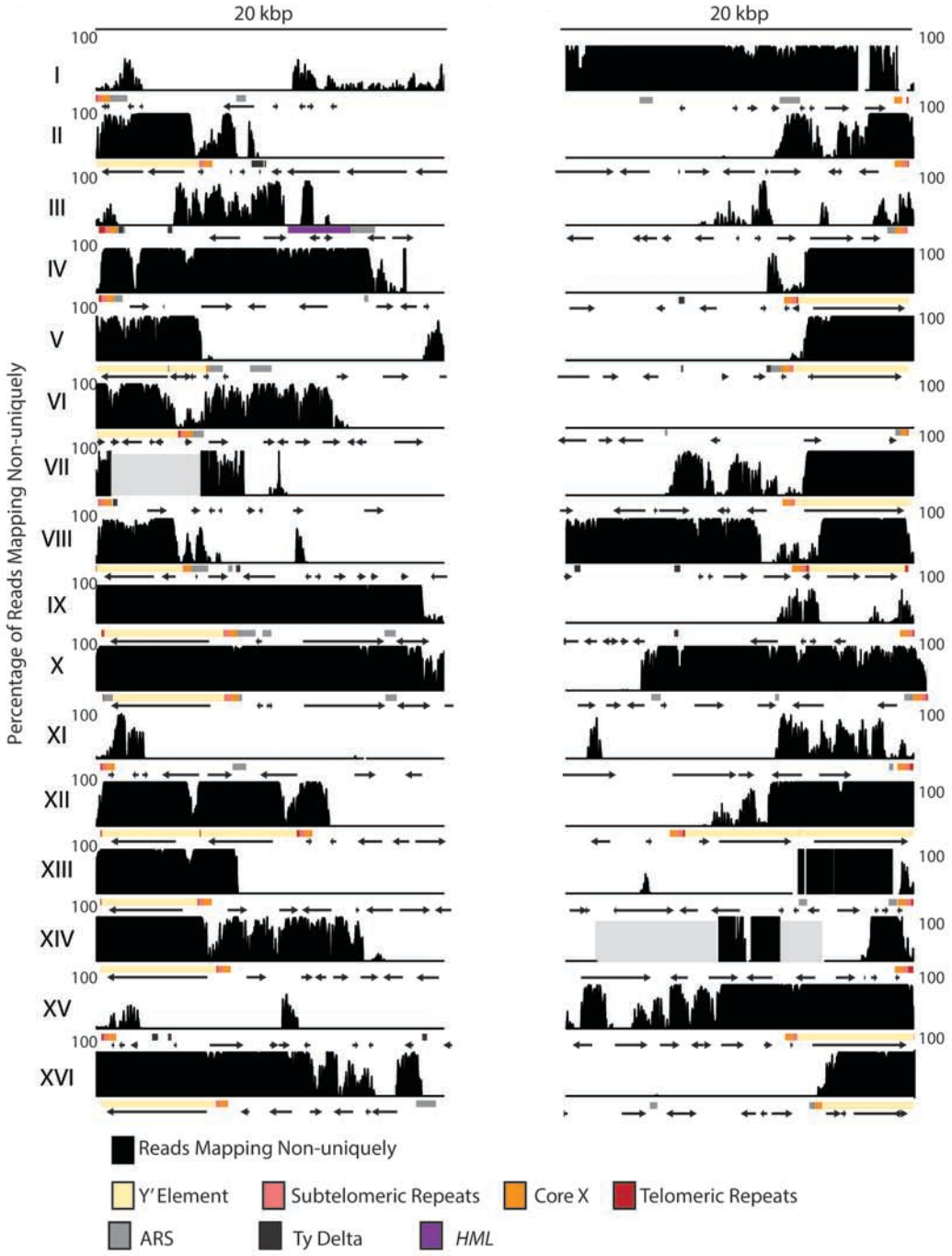

Figure S3. **Percentage of non-uniquely mapping reads from ChIP-Seq experiments at all thirty-two telomeres.** Reads that mapped non-uniquely in the Sir4 input dataset from (THURTLE and RINE 2014) were determined by those reads with a MAPQ flag of 0. The number of reads that mapped non-uniquely at that base-pair position was determined and divided by the total number of reads that mapped at that position. This percentage of non-uniquely mapped reads was plotted for each telomere. 20 kbp for each telomere is shown. Salient features as annotated in SGD are indicated below the X-axis for each telomere as in Figure 2. The light gray rectangles indicate regions deleted in the sequenced W303 derived lab strain relative to the SGD sacCer2 reference genome.

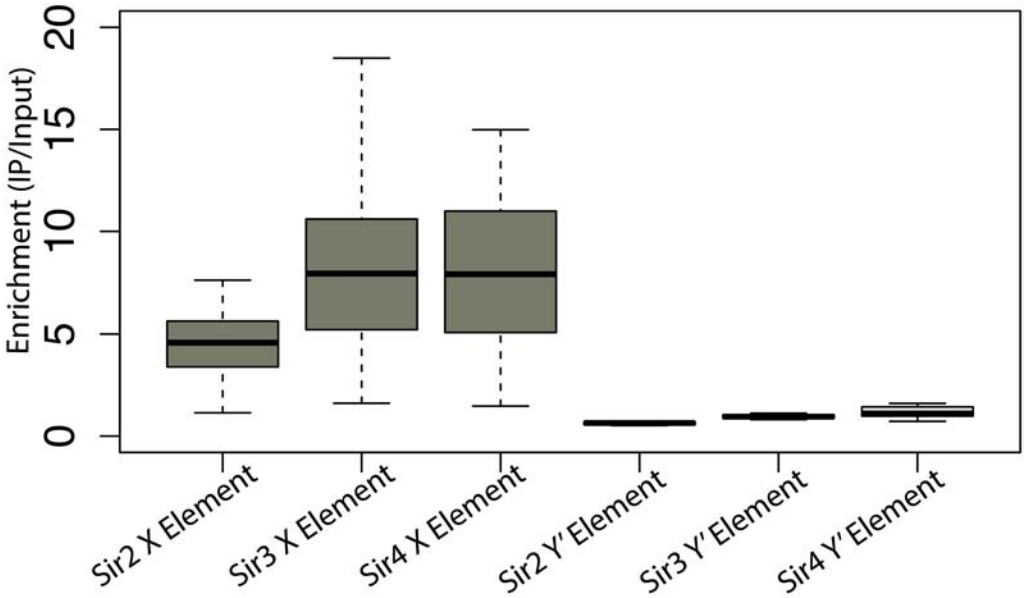

Figure S4. Sir proteins are not enriched at Y' elements. Average enrichment for all annotated X elements and Y' elements was calculated for all three Sir proteins. Enrichment was determined by the average IP/Input for that sample for the X elements and Y' elements for each chromosome as defined in SGD.

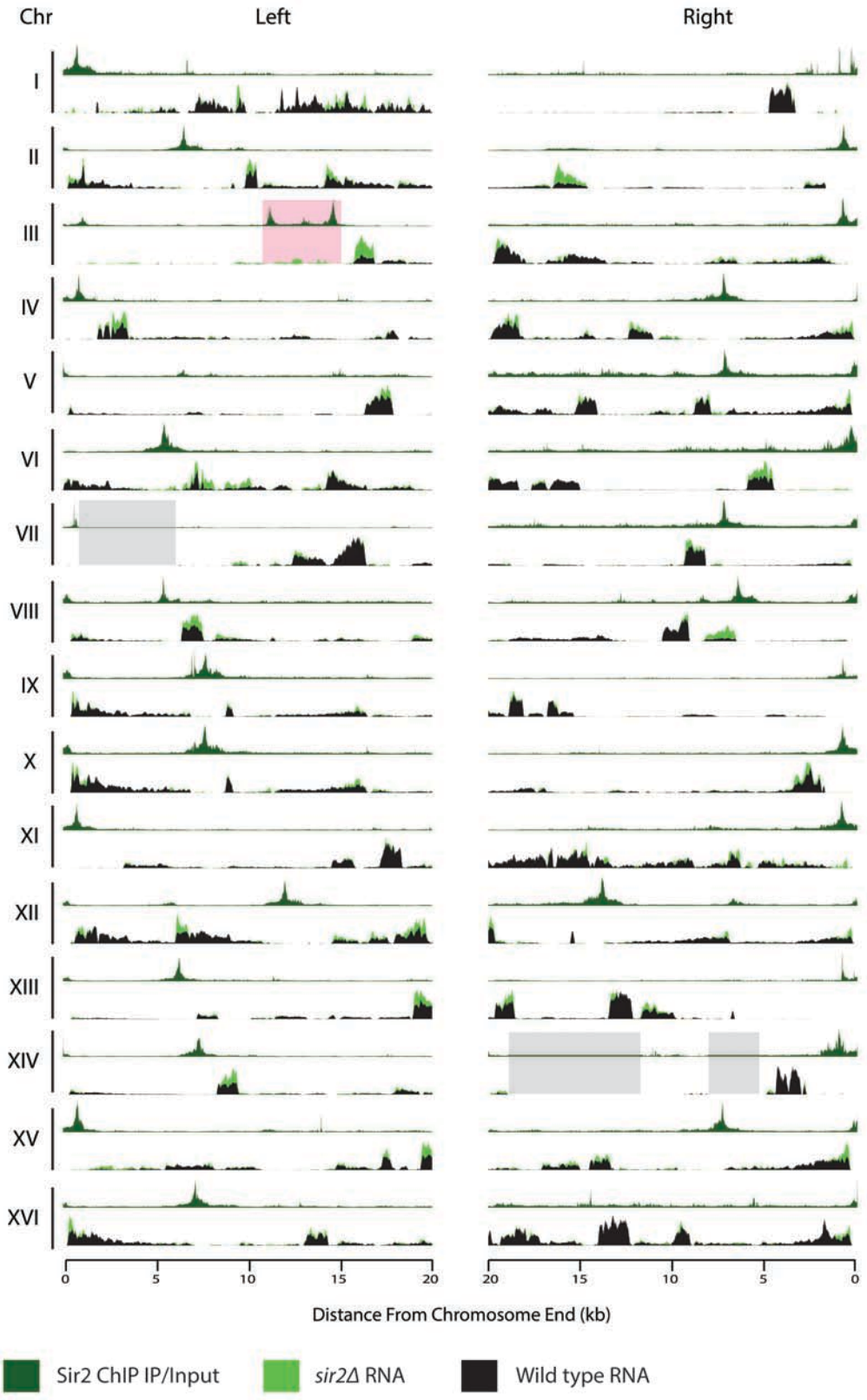

Figure S5. Transcription occurs in subtelomeric genes adjacent to peaks of Sir2 protein. For each telomere arm, top axis shows Sir2 IP/input (dark green) and lower axis shows transcription in the form of RNA read pileups in wild type (black) *sir2Δ* (light green).

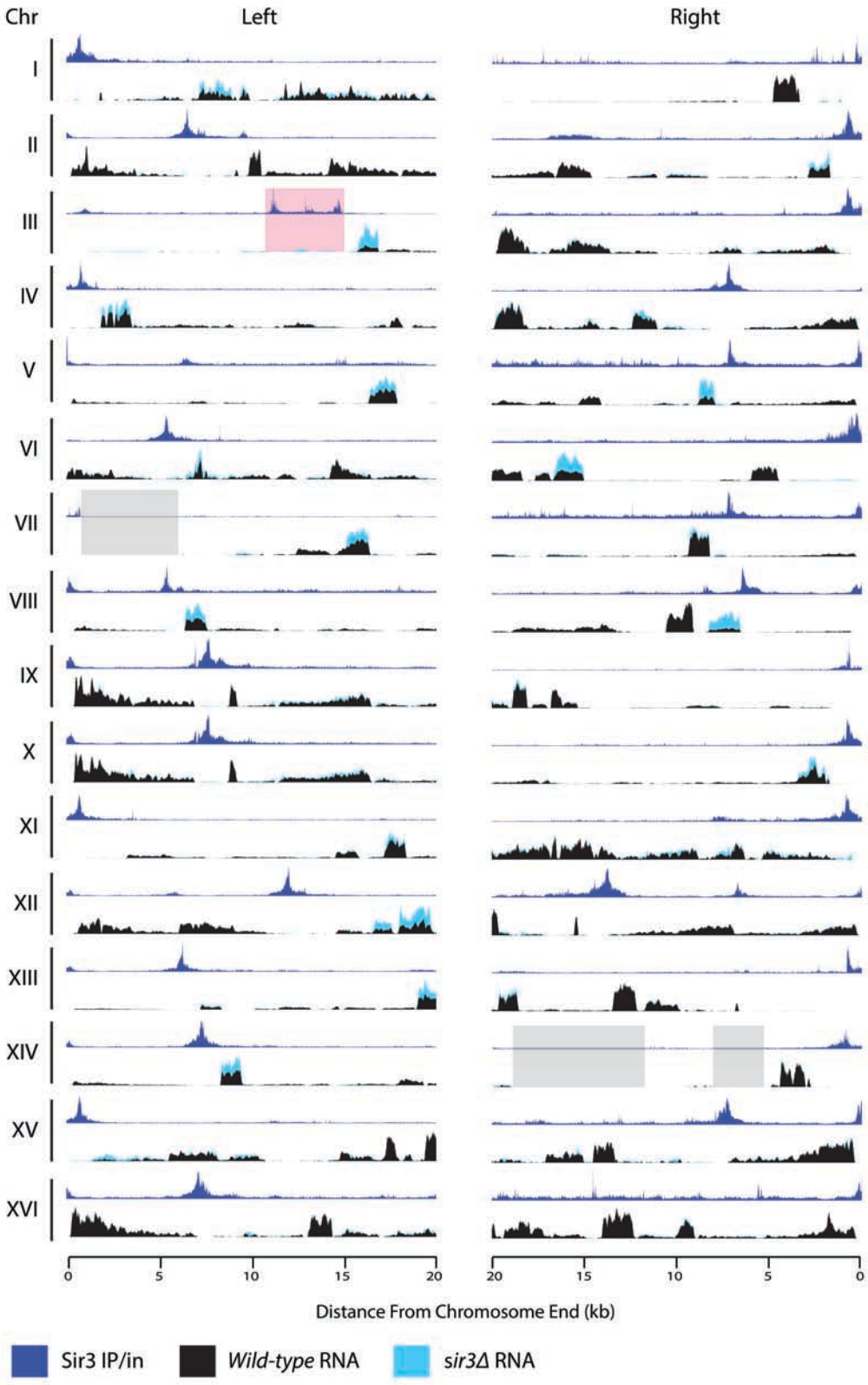

Figure S6. A comparison of Sir3 protein association and expression in wild type *sir3Δ*. For each telomere arm, top axis shows Sir3 IP/input (dark blue) and lower axis displays transcription as RNA read pileups in wild type (black) and *sir3Δ* (light blue).

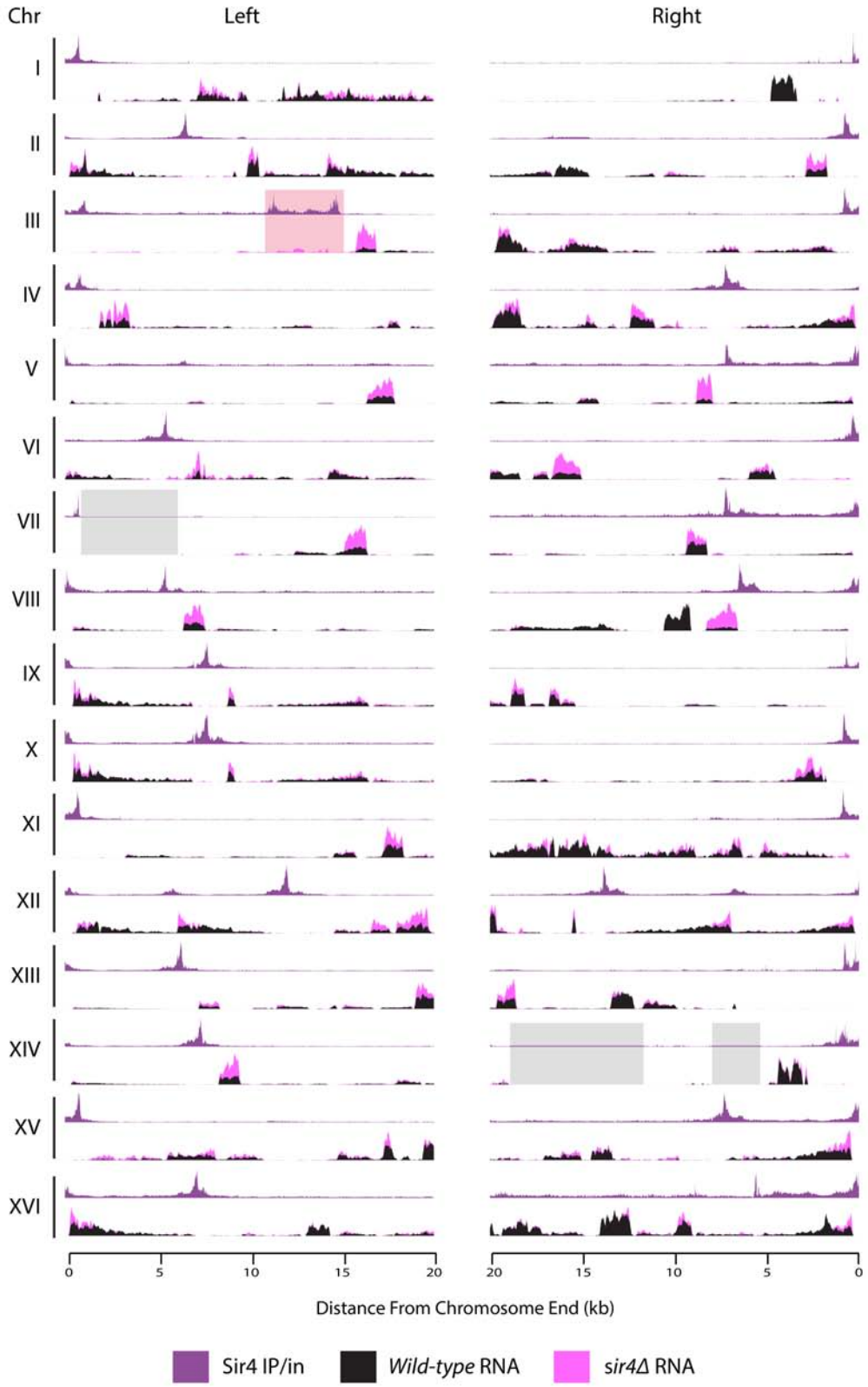

Figure S7. Comparison of Sir4 protein association and expression in wild type and *sir4Δ*. For each telomere arm, top axis shows Sir4 IP/input (dark purple) and lower axis shows transcription as RNA read pileups in wild type (black) and *sir4Δ* (pink).

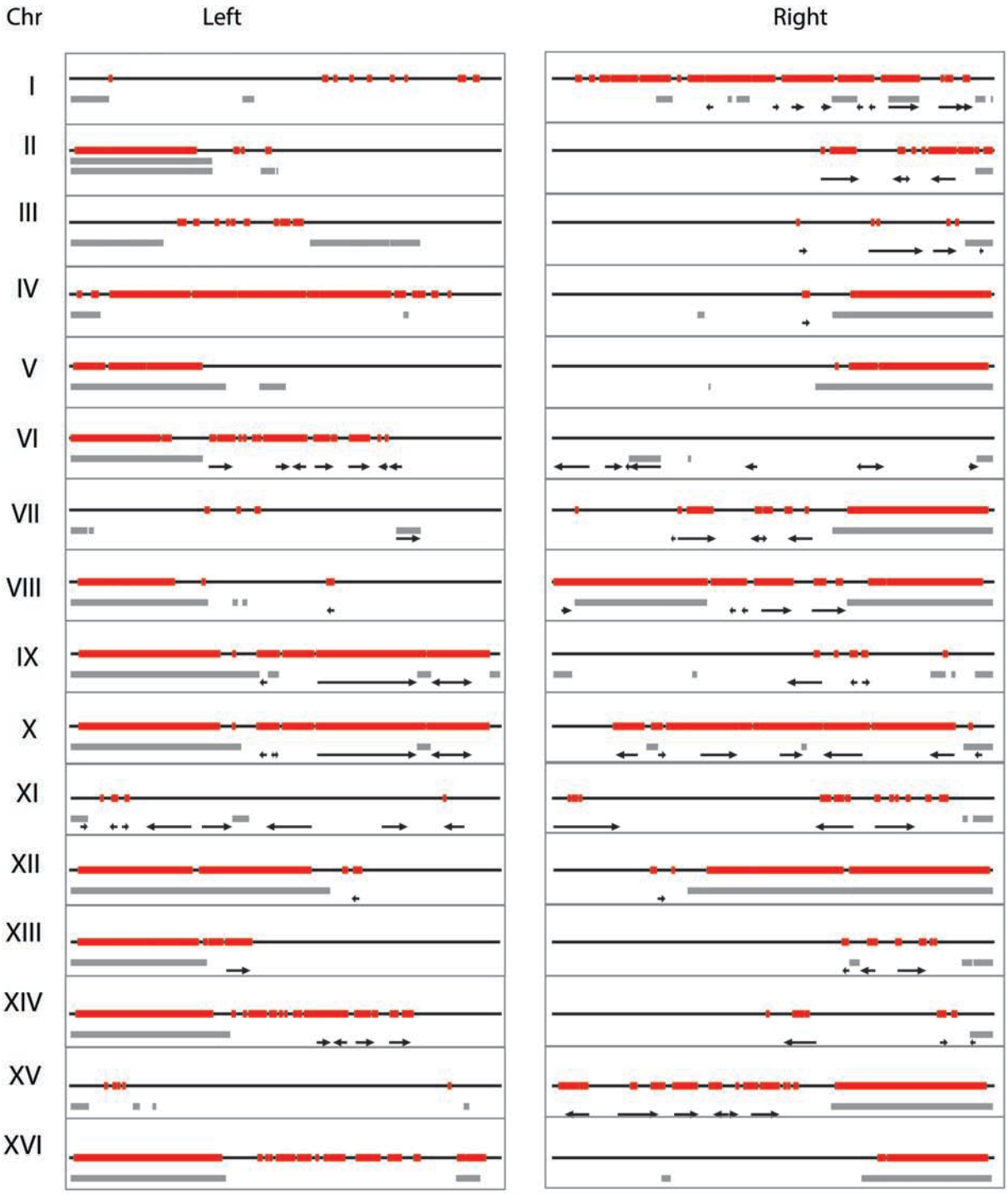

Figure S8. Positions of non-uniquely mapping reads across all thirty-two telomeres from RNA-Seq experiments. Shown in red are regions of all thirty-two telomeres that contribute non-non-uniquely mapping reads in RNA-Seq experiments. Positions of annotated Y' elements, Ty δ elements, telomeric repeats, and X elements are shown in gray boxes. Black arrows depict ORFs.